Color Imaging for Multimedia

GAURAV SHARMA, MEMBER, IEEE, MICHAEL J. VRHEL, MEMBER, IEEE, AND H. JOEL TRUSSELL, FELLOW, IEEE

To a significant degree, multimedia applications derive their effectiveness from the use of color graphics, images, and video. However, the requirements for accurate color reproduction and for the preservation of this information across display and print devices that have very different characteristics and may be geographically apart are often not clearly understood. This paper describes the basics of color science, color input and output devices, color management, and calibration that help in defining and meeting these requirements.

***Keywords*—** *Color, color imaging, colorimetry, display, multimedia, printing, scanning, survey, tutorial.*

I. INTRODUCTION

In the last few years, computer-based multimedia systems have grown from their humble beginnings into systems that truly allow the integration of information from many different types of sources (media), including text, numeric data, audio, graphics, still images, and video. In keeping with this trend, it is anticipated that multimedia systems will continue to grow rapidly in the areas of information presentation, education, and entertainment, with applications including teaching, electronic publishing, telemedicine, and retailing. In the initial euphoria surrounding these developments, however, several issues have not received adequate attention. In particular, for the presentation of image data, one question is still left over from the early days. How do you ensure that two images presented on two different devices can be accurately compared?

The problem is much more complex now than in early systems. Images that are to be compared in present multimedia applications may come from entirely different input sources and may be reproduced on entirely different output devices. Consider the publisher of a merchandise catalog who is trying to sell products over the World Wide Web. The images of the products may come from photographic film, from digital still cameras, or even from camcorders. The images that are produced for the customer may be viewed in a printed catalog or on the computer monitor or downloaded and printed on the user's local printer. To avoid unnecessary grief to the customer, the final image in all cases should be a faithful representation of the original product. Other examples could be given for remote medical diagnosis, educational presentations, industrial design of products, and, of course, entertainment.

Since color is such a large part of multimedia presentation, it is important that both the designers and users of multimedia systems understand how to describe and present color accurately. The presentation of accurate color requires a joint effort on the part of both the designer or manufacturer and the consumer. The consumer should be aware of the need for the calibration of both input and output devices. The designers of imaging devices for multimedia systems should make their devices easy to calibrate and easy to maintain calibration. At the same time, designers of multimedia applications should make products that effectively use the calibration of the various devices.

There is a range of needs of the users that must be spanned by the producers of multimedia products. The level of color accuracy required for an application must be identified in order to specify what hardware can be used and what information is to be given or supplied by the user. In the case of accurate color presentation, it is often important to know the intent of the user of the image. In certain applications, such as mail-order catalogs, absolute colorimetric accuracy is desired so that chosen items may match or coordinate with existing articles. In other applications, such as presentation of art on a computer, it is often necessary to sacrifice absolute colorimetric accuracy in favor of an image that appears visually similar to that in the museum, under the much different viewing conditions of the monitor. To achieve either of these effects, the original image must be recorded correctly so that the data can produce a good display. Information about the rendering intent (for instance, colorimetric versus perceptual) for displaying the image must also be tagged to the image file for interpretation and use in a display device.

As can be seen from this brief introduction, there are several steps to producing good color images for a mul-

Manuscript received August 15, 1997; revised December 1, 1997. The Guest Editor coordinating the review of this paper and approving it for publication was A. M. Tekalp.

G. Sharma is with the Digital Imaging Technology Center, Xerox Corporation, Webster, NY 14580 USA (e-mail: sharma@wrc.xerox.com).

M. J. Vrhel is with Color Savvy Systems, Ltd., Springboro OH 45066 USA (e-mail: mvrhel@colorsavvy.com).

H. J. Trussell is with the Electrical and Computer Engineering Department, North Carolina State University, Raleigh, NC 27695-7911 USA (e-mail: hjt@eos.ncsu.edu).

Publisher Item Identifier S 0018-9219(98)03520-8.

timedia application. This paper presents the fundamentals that both the user and the designer should understand in order to get the most from the system. Section II describes the basics of the color visual system, color terminology, and color relationships. The third section has three major subtopics that are closely interrelated. Image characteristics and reproduction methods are discussed together, since many images used in multimedia presentations are themselves reproductions of other images. Image-recording methods are dependent on the characteristics of the image. Section IV presents the basics of color management and calibration, which are necessary to communicate color information among the various devices. Section V details an illustrative example that uses the principles described, and Section VI gives a summary of the paper. At the outset itself, the authors would like to clarify that to keep the paper brief, they have attempted to select a few representative citations instead of attempting exhaustive coverage and duly assigning credit.

II. Color Vision and Colorimetry

The perception of color involves complex interactions between several physical, neural, and cognitive phenomena, which must be understood in order to comprehend color vision completely. While research is still ongoing in the integration of all these aspects of color, significant success has been achieved in understanding the physical and (to a lesser extent) neural phenomena involved in color sensation. The goal of this section is to present an overview of this current understanding, with particular emphasis on the aspects that are of interest in color-imaging applications.

A. Trichromacy and the Visual Subspace

The sensation of color is produced when light in the visible region of the electromagnetic spectrum (approximately corresponding to the wavelength region from 400 to 700 nm) excites retinal receptors in the eye. The human eye has three color-sensing receptors, called S, M, and L cones, which are abbreviated forms of short-, medium-, and long-wavelength sensitive cones, respectively. Under a fixed set of viewing conditions, the response of these cones can be accurately modeled by a linear system defined by the spectral sensitivities of the cones. For the purposes of this paper, it will be convenient to assume that (color) spectra are represented by N-vectors consisting of their samples at a discrete set of wavelength values $\lambda_1, \lambda_2, \cdots \lambda_N$ that span the visible wavelength range. Thus, the cone responses produced by light (stimulus) with spectral power distribution $\mathbf{f}$ are given by

$$\mathbf{c} = \mathbf{S}^T\mathbf{f} \tag{1}$$

where $\mathbf{c} = [c_1, c_2, c_3]$ is the vector of cone responses and $\mathbf{S} = [\mathbf{s}_1, \mathbf{s}_2, \mathbf{s}_3]$ is the $N\times$ 3 matrix of cone spectral sensitivities.

Equation (1) was first inferred from experimental observations of the linearity of color matching and the phenomenon of *trichromacy*, which states that it is possible to produce a color match for a given stimulus (equivalently, identical cone responses under the same viewing conditions) by using only three light sources, known as *primaries* (see [1] and [2] for references and a description using notation and terminology identical to that used here). The sensitivity functions, however, have been subsequently verified through physiological examinations. From (1), it can be seen that the cone responses depend only on the orthogonal projection of the spectrum $\mathbf{f}$ onto the column space of $\mathbf{S}$, which is called the human visual subspace (HVSS) [3]–[6].

While the cone sensitivities $\mathbf{S}$ themselves cannot be readily determined, alternate bases that span the HVSS can be determined through color-matching experiments that determine the strengths of primaries required to match monochromatic color spectra over the entire visible range [1], [2], [7]. These bases are known as color-matching functions (CMF's) and depend on the primaries used in the color-matching experiments. The $N\times$ 3 matrix formed by a set of CMF's is within a (nonsingular) linear transformation of $\mathbf{S}$. Out of the infinite set of CMF's that can be used for color specification, the International Commission on Illumination (CIE) has defined two sets of CMF's for use in standard colorimetry: 1) the CIE red-green-blue (RGB) CMF's and 2) the CIE XYZ CMF's [8]. The CIE RGB CMF's correspond to monochromatic primaries at 700 nm (red), 546.1 nm (green), and 435.8 nm (blue). The CIE XYZ CMF's do not correspond to any physical set of primaries but were selected by the CIE so as to have several properties that were considered desirable when the standards were defined [9], [10, p. 531]. In this paper, the CIE XYZ CMF's will be used. Using these CMF's, the color of the irradiant spectrum $\mathbf{f}$ can be specified by its CIE XYZ tristimulus value, which is given by $\mathbf{t} = \mathbf{A}^T\mathbf{f}$, where $\mathbf{A} = [\mathbf{a}_1, \mathbf{a}_2, \mathbf{a}_3]$ is a matrix whose columns are the CIE XYZ CMF's. Since the results of color-matching experiments vary in accordance with the angular size of the viewing field, the CIE has defined two sets of XYZ CMF's: 2° CMF's for use with uniform visual fields of angular subtense from 1° to 4° and 10°CMF's for use with uniform visual fields of larger angular subtense. Only the 2° CMF's will be used throughout this paper because imaging applications involve complex visual fields where the color-homogeneous areas have small angular subtense. The (2°) CIE XYZ CMF's are shown in Fig. 1. The perceived lightness/brightness of a color is often assumed to be a monotonic function of the Y tristimulus value, which is known as the *luminance*; and the corresponding CMF, $\bar{y}(\lambda)$, is often referred to as the photopic luminosity function.

As mentioned earlier, the 3 $\times N$ matrices $\mathbf{A}$ and $\mathbf{S}$ are within a (nonsingular) linear transformation of each other. Therefore, the HVSS can alternately be defined as the column space of $\mathbf{A}$. Also note that for colorimetry in specific applications, alternate standard CMF's have also been defined, an example being the National Television Systems Committee (NTSC) [11]/Society for Motion and Television Pictures (SMPTE) [12], [13] CMF's developed for use in TV. The same color can therefore be specified

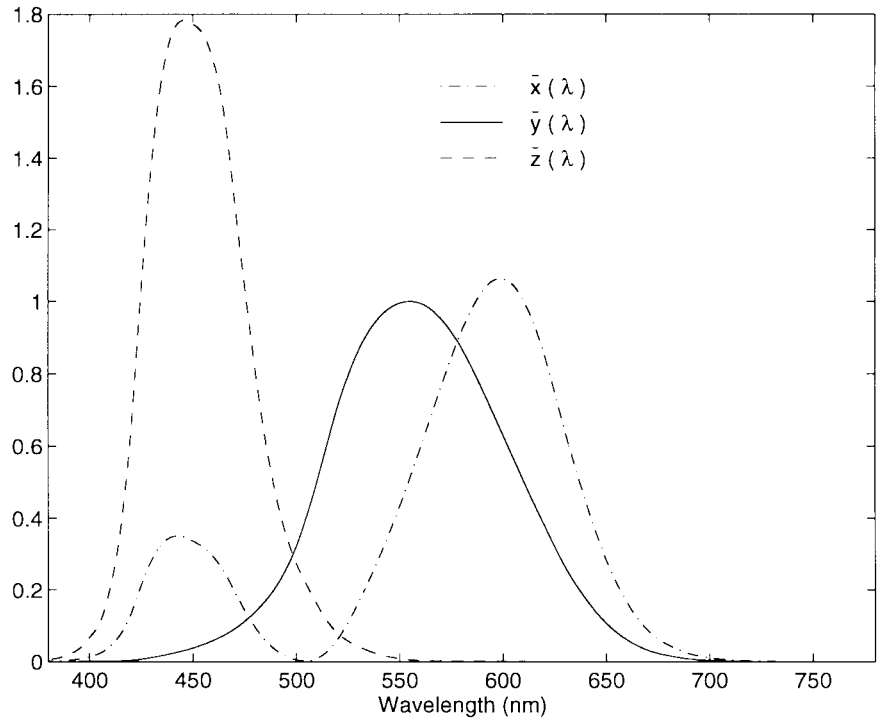

Fig. 1. CIE 2° XYZ color-matching functions.

in numerous *color spaces* by using tristimulus values computed with these different CMF's. The term "color space" is also applied to other coordinate systems used for specifying color, which are typically transformations of the tristimulus values.

B. Colorimetry for Reflective Objects

The discussion in the last section was based on the assumption that $\mathbf{f}$ is the spectral irradiance of the light incident on the eye. When a reflective object with spectral reflectance $\mathbf{r}$ is viewed under an illuminant with spectrum given by the N vector $\mathbf{l}$, the resulting spectral radiance at the eye is the product of the illuminant spectrum and the reflectance at each wavelength. Therefore, the CIE XYZ tristimulus value defining the color is given by

$$\mathbf{t} = \mathbf{A}^T\mathbf{L}\mathbf{r} = \mathbf{A}_\mathbf{L}^T\mathbf{r} \tag{2}$$

where $\mathbf{A}$ is the matrix of CIE XYZ CMF's (as before), $\mathbf{L}$ is the diagonal illuminant matrix with entries from $\mathbf{l}$ along the diagonal, and $\mathbf{A_L} = \mathbf{LA}$. Color measurement for transmissive objects can be similarly defined in terms of their spectral transmittance. In analogy with the HVSS, the column space of $\mathbf{A_L}$ is defined as the *human visual illuminant subspace* [6]. Note that (2) is a simplified model of the interaction between the illuminant and the surface that does not account for several geometry/surface effects. In particular, the reflected light from a surface typically has a specular component (similar to reflection by a mirror) in addition to the diffuse component represented in (2). Throughout this paper, it will be assumed that the specular component is excluded from the color-measurement process. This assumption is normally valid for the measurement geometries used in common color instrumentation. An additional limitation of (2) is its inability to account for fluorescence.

Note that the linear model of (1) and (2) (or any equivalent model) is limited in several respects. While this model usually explains the color matching of two spatially uniform patches placed over a constant background, it does not take into account several adaptation effects in the eye that are inherently nonlinear [14, ch. 9]. As will be discussed in Section II-D1, the simple linear model does not completely explain even the matching of uniform patches of color under different viewing conditions, let alone the color-matching characteristics of complex scenes. An additional limitation of the linear model, which will also be addressed in Section II-D1, is that Euclidean distances in the tristimulus spaces defined by the model are in poor agreement with perceived color differences.

C. Illuminants and Color Temperature

The tristimulus color specification of a reflective object is dependent on the viewing illuminant. The CIE has defined several standard illuminants for use in colorimetry of reflective objects. The relative irradiance spectra of a number of these standard illuminants is shown in Fig. 2. To represent different phases of daylight, a continuum of daylight illuminants has been defined by the CIE [8], which are uniquely specified in terms of their *correlated color temperature* (CCT). Since the temperature of a black-body radiator describes its complete spectral power distribution and thereby its color, it is commonly referred to as the color temperature of the black body. For an arbitrary illuminant, the CCT is defined as the color temperature of the black-

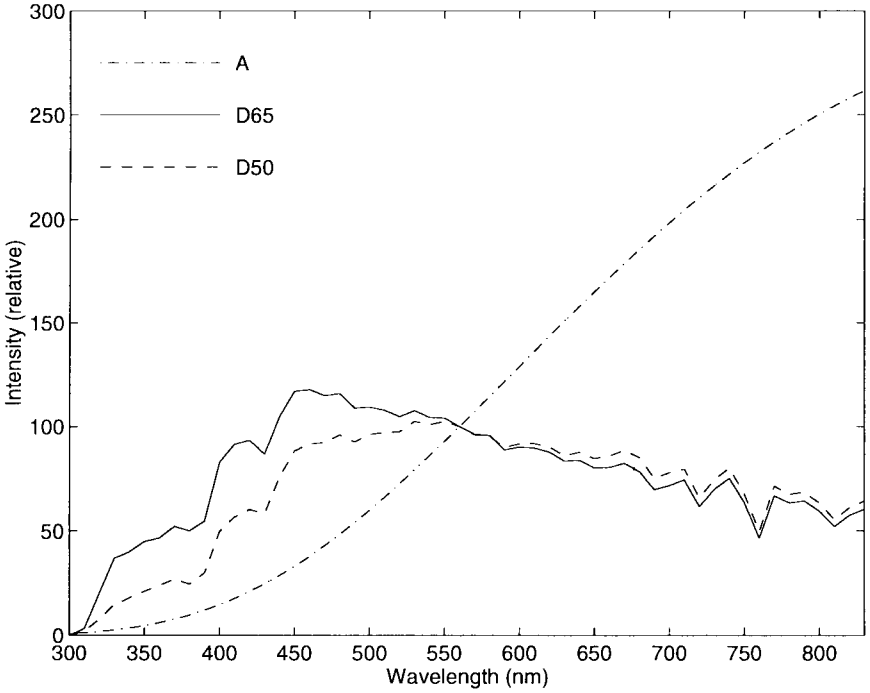

Fig. 2. CIE standard illuminants.

body radiator that is visually closest to the illuminant (in color) [7]. The D65 and D50 illuminant spectra shown in Fig. 2 are two daylight illuminants commonly used in colorimetry, which have CCT's of 6500 and 5000 K, respectively. The CIE illuminant "A" represents a blackbody radiator at a temperature of 2856 K and closely approximates the spectra of incandescent lamps. Sources with lower CCT tend to be more red, while those with higher temperatures are bluer. Illuminants with similar CCT are assumed to be similar with regard to their color rendering of illuminated objects. This, however, is true only for illuminants whose spectra closely resemble that of a blackbody radiator, and other spectra that have identical CCT can have very different distributions and color-rendering properties [15]. An example of the problem with the use of CCT for specifying the color-rendering properties of an illuminant is shown in Fig. 3, where two synthesized illuminants are shown along with a reflectance spectrum measured from a cyan print sample. Though the illuminants have the same luminance and an identical CCT of 5000 K, the color difference for the reflectance sample under the two illuminants is rather large, corresponding to 44.4 ΔE^*_{ab} units. (For the definition of ΔE^*_{ab} see Section II-D1.)

D. Psychophysical Aspects of Color

The simple model of (1) describes only a small part of the complex color-perception process. In particular, the cone responses cannot be directly related to the common color attributes of *hue, saturation,* and *lightness/brightness*.[1] The outputs of the cones go through a process of nonlinear transformation and mixing in the neural pathways leading from the eye to the brain. It is believed that this process transforms the cone responses into an achromatic channel carrying only information of lightness/brightness and two opponent chromatic channels: one carrying a red-green chromatic-difference signal and the other carrying a yellow-blue chromatic-difference signal. Research has indicated that the achromatic channel carries information at a high spatial resolution and the chromatic channels use significantly reduced resolution. This framework for color vision is broadly accepted and is successful in qualitatively explaining a wide variety of observations from psychophysical experiments. However, the exact nature of the transformations involved is still the subject of active research. The interested reader is referred to [10] and [14] for recent descriptions and historical references. Several semiempirical models that conform to the above framework have been developed for use in color science and imaging.

1) Uniform Color Spaces and Color Appearance: One limitation of the CIE XYZ space (and other tristimulus spaces) is that it is perceptually nonuniform, i.e., equal differences in CIE XYZ tristimulus values (as measured by the Euclidean distance) do not correspond to equal perceived differences in colors. Thus, the CIE XYZ space is primarily useful for determining color matches and not the closeness of colors that are not in exact match. Since a measure of the perceived difference between colors is very useful in many applications, considerable research has focused on transforming tristimulus values into alternate color spaces that are perceptually uniform. The CIE has defined two uniform color spaces (UCS's) for use in colorimetry, of which the more commonly used is the CIELAB color space

[1] The readers are referred to [7, pp. 487] and [16]–[18] for definitions of hue, saturation, lightness, brightness, and other color-appearance terminology. Common notions of these terms, however, will suffice for the purposes of this paper.

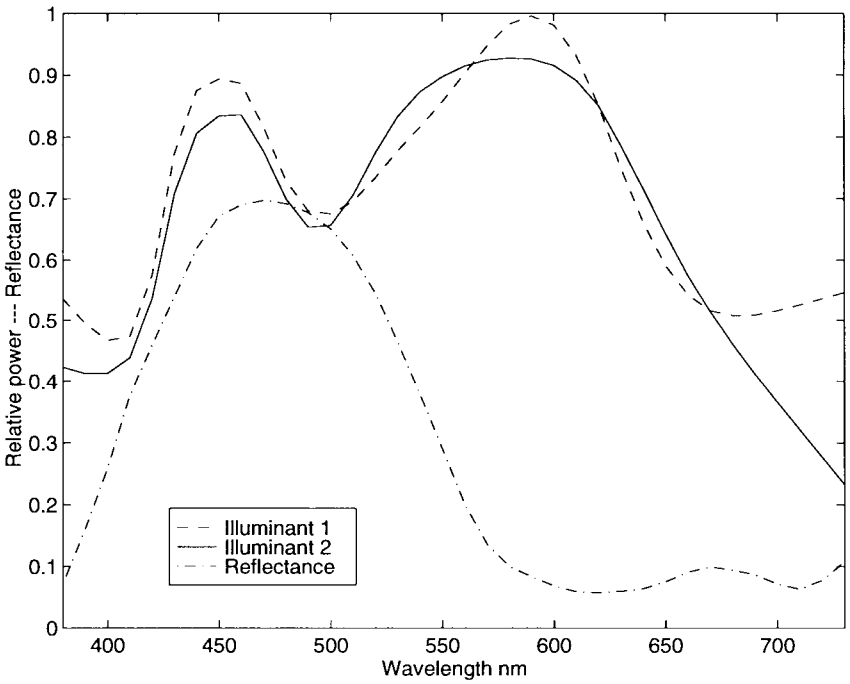

Fig. 3. CCT counterexample with two illuminants, with CCT $= 5000$ K and a spectral reflectance.

[8]. The CIELAB color space is based on a color vision model [19] and transforms XYZ tristimulus values into an achromatic lightness value L^* and two chromatic values a^* and b^* using the transformations

$$\begin{aligned} L^* &= 116 f\left(\frac{Y}{Y_n}\right) - 16 \\ a^* &= 500\left(f\left(\frac{X}{X_n}\right) - f\left(\frac{Y}{Y_n}\right)\right) \\ b^* &= 200\left(f\left(\frac{Y}{Y_n}\right) - f\left(\frac{Z}{Z_n}\right)\right) \end{aligned} \tag{3}$$

where X_n, Y_n, Z_n are the tristimuli of the "white stimulus" and

$$f(x) = \begin{cases} x^{\frac{1}{3}} & x > 0.008856 \\ 7.787x + \frac{16}{116} & x \le 0.008856. \end{cases} \tag{4}$$

The chromatic channel a^* is a red-green opponent channel in that positive values for a^* indicate redder colors and negative values indicate greener colors, with the magnitude indicating the strength of the redness/greenness. Similarly, b^* is a yellow-blue opponent color channel. Note that the lightness value L^* depends on only the luminance Y, and this is a result of a deliberate decision made in choosing the CIE XYZ CMF's.

The Euclidean distance between two color stimuli in CIELAB space is denoted by ΔE^*_{ab} (delta E-ab), and a ΔE^*_{ab} value of around 2.3 corresponds to a just noticeable difference [20]. The radial distance ($\sqrt{(a^*)^2 + (b^*)^2}$) and angular position ($\arctan(\frac{a^*}{b^*})$), in the a^*b^* plane, serve as correlates of chroma and hue, respectively. Thus, a transformation of CIELAB into cylindrical coordinates provides approximate lightness, chroma, and hue attributes. This is extremely useful in applications that require color data to be manipulated along these perceptual axes. In addition, this transformation has been exploited in defining alternate (non-Euclidean) color-difference formulas in CIELAB space that attempt to remedy the deviations from uniformity in CIELAB. Most of these formulas decompose the total CIELAB color difference into lightness, hue, and chroma differences and introduce weighting factors for these differences that are determined by the lightness, hue, and chroma. The weighting factors are determined so as to obtain better agreement of the modified color-difference formula with experimental data. The most prominent and successful among these difference formulas is the CMC(l:c) distance function [21]. Recently [22], the CIE issued a new recommendation for the computation of color differences in CIELAB space that incorporates several of the robust and attractive features of the CMC(l:c) distance function. Color differences computed in accordance with this recommendation are referred to as ΔE^*_{94} color differences.

The human eye can sense color over a very large dynamic range of light intensities. One of the remarkable aspects of color vision is that the color of reflective objects is largely unchanged over this vast range of light intensities and over several different viewing illuminants. The term *color constancy* is used to describe this phenomenon of object colors' remaining invariant under changes in viewing illumination. The adaptation of the color-sensing mechanism in the eye in response to these changes is called *chromatic adaptation*. Obviously, this chromatic adaptation is not included in the simple linear model of (1), which works only for a fixed set of viewing conditions. Most models of chromatic adaptation assume that it is achieved through independent adaptive gain control on each of the three cones. This approach was first proposed by Von Kries [23], who hypothesized that the cone responses are scaled linearly so that the

white stimulus produces the same response under different viewing conditions. Mathematically, this is achieved by applying a diagonal scaling matrix to the cone responses and is referred to as a Von Kries transformation [7]. Note that the white normalization of the XYZ tristimuli in the transformation to CIELAB in (3) is motivated by the same reason, though the transformation is not really a Von Kries transform because the XYZ tristimuli are not cone responses. As will be discussed in Section IV-E, a Von Kries transform is often used in imaging applications to account for the eye's adaptation to changes in viewing conditions.

Several researchers are investigating models for color vision that incorporate adaptation and other psychophysical effects and provide descriptors of color appearance that are independent of the viewing conditions (as opposed to simple CIE XYZ colorimetry). These *color-appearance* models hold great promise in imaging applications that require images to be rendered on different devices (such as a CRT monitor and print) with different viewing conditions. To obtain "identical appearing images," the input viewing conditions and the colorimetric specification of the image under these viewing conditions are used in a color-appearance model to obtain a color-appearance description of the image. The color-appearance description, along with the output viewing conditions, can then be used in the inverse of the appearance model to obtain the colorimetry (under the output viewing conditions) for an image that appears identical to the input image. The reader is referred to [24] for a survey and comparison of several of the current color-appearance models.

2) Spatial Aspects: The CIELAB color space attempts to account for the nonlinearities in the color-sensing process for the comparison of relatively large uniform color regions and does not account for any spatial interactions in the eye. Since the eye acts as a spatial low-pass filter, which can average over high spatial-frequency differences in images, a point-by-point computation of color differences in CIELAB color space is not appropriate for the comparison of images. Though the eye exhibits low-pass characteristics for both luminance[2] and chrominance spatial information, the bandwidth for the chrominance channels is much lower than that of the luminance channels. This fact has been exploited in numerous applications, including color television (TV), where the transmission bandwidth allocated to the chrominance channels is significantly lower than that for the luminance channel.

Several researchers have modeled the spatial properties of the eye as a linear filter and studied the frequency response of the eye for luminance and chrominance spatial patterns [25], [26]. However, a complete model for human vision that is perceptually uniform and incorporates the effects of the spatial interactions is yet to be developed. Recent attempts in this direction include the S-CIELAB model [27] that builds on CIELAB by incorporating spatial low-pass filters for the L^*, a^*, and b^* channels. Similar approaches based on slightly different transforms for luminance and chrominance channels have also been proposed in [26], [28], and [29]. While other models that are considerably more sophisticated have been developed for luminance information [30], [31], their extensions to color are yet to be developed.

[2] Strictly speaking, the luminance response of the eye is believed to be bandpass, but for all practical purposes, the low-frequency attenuation can be ignored.

III. Color-Image Reproduction and Recording Devices

In the physical world, color images exist as spatially varying spectral radiance or reflectance distributions. To be processed digitally, these images need to be sampled both spatially and spectrally. The issues involved in spatial sampling and reconstruction of images have been discussed at length in signal-processing literature and will not be repeated here. The aspects of spectral sampling and color recording for images will be discussed here. Common color-reproduction devices, spectral characteristics of natural images and images from these reproduction devices, and methods for recording these images are described briefly.

A. Image-Reproduction Systems

There are several systems that are commonly used for the reproduction of color images. These systems can be broadly classified into three types: *additive, subtractive,* and *hybrid*. Additive color systems produce color through the combination of differently colored lights, known as primaries. The qualifier additive is used to signify the fact that the final spectrum is the sum (or average) of the spectra of the individual lights. Examples of additive color systems include color cathode-ray tube (CRT) displays and projection video systems. Color in subtractive systems is produced through a process of removing (subtracting) unwanted spectral components from "white" light. Typically, such systems produce color on transparent or reflective media, which are illuminated by white light for viewing. Dye sublimation printers, color photographic prints, and color slides are representatives of the subtractive process. Hybrid systems use a combination of additive and subtractive processes to produce color. The main use of a hybrid system is in color halftone printing, which is commonly used for lithographic printing and in most desktop color printers.

Any practical output system is capable of producing only a limited range of colors. The range of producible colors on a device is referred to as its *gamut*. Typical additive systems use red, green, and blue primaries because they offer the largest possible gamut, and for the same reason, subtractive systems use cyan (C), magenta (M), and yellow (Y) colorants. In addition, subtractive systems often use a fourth black (K) colorant in addition to CMY to achieve greater contrast, better reproduction of achromatic (gray) colors, and lower cost through the replacement of the more expensive CMY colorants with the K.

The gamut of a device can be represented by a three-dimensional (3-D) solid in any color space such as CIE XYZ/CIELAB. Since two-dimensional (2-D) representations are more convenient for display, it is common to

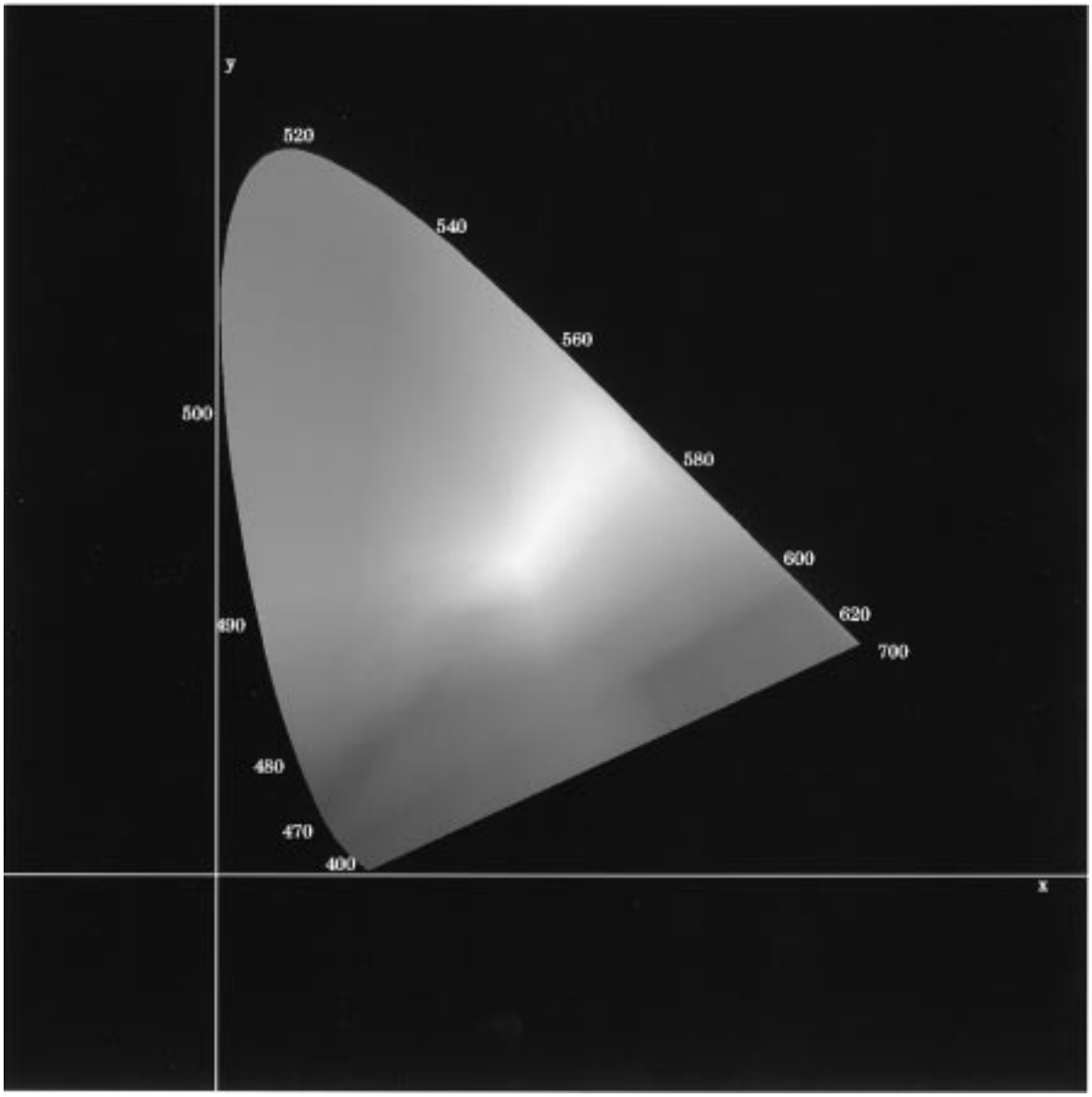

Fig. 4. CIE xy chromaticity diagram showing locations of colors in chromaticity space.

utilize CIE xy chromaticity diagrams [7] for this purpose, where the x and y chromaticity coordinates are $X/(X+Y+Z)$ and $Y/(X+Y+Z)$, respectively. A graphical representation of the CIE xy diagram showing the relative locations of the different colors is displayed in Fig. 4. [32] On the CIE xy chromaticity diagram, the gamut of an additive system appears as a convex polygon with the primaries representing the vertices. For the usual case of three red, green, and blue primaries, the gamut is a triangle on the CIE xy chromaticity diagram. Since most subtractive and hybrid systems are nonlinear, their gamuts have irregular shape and are not characterized by such elegant geometric constructs. The two-dimensional representation of the gamut on the CIE xy diagram presents only an incomplete (and difficult to interpret) picture because it does not represent the full 3-D data. With the increase in computing speeds and advances in computer graphics, visualization techniques are now used to render 3-D views of the gamuts [33], [34]. The ability to manipulate these views interactively is extremely useful in understanding the capabilities and limitations of the different color-output devices. Three different views comparing the gamuts of a CRT monitor and the gamut of a dye-sublimation contone color printer are shown in Fig. 5, and identical views for an inkjet halftone color printer are shown in Fig. 6. In both cases, the wire frames represent the gamut of a CRT monitor and the solids represent the gamuts of the printer. These views demonstrate that the gamuts of these three output devices are fairly different with several colors that can be produced on one device and not on another. Overall, the gamut of the monitor is the largest, followed by the gamut of the continuous-tone printer and then by the inkjet halftone printer, which has a rather small gamut in comparison to the other devices. As will be seen in Section IV-D, this mismatch in the gamut between the devices poses significant challenges in cross-media color reproduction.

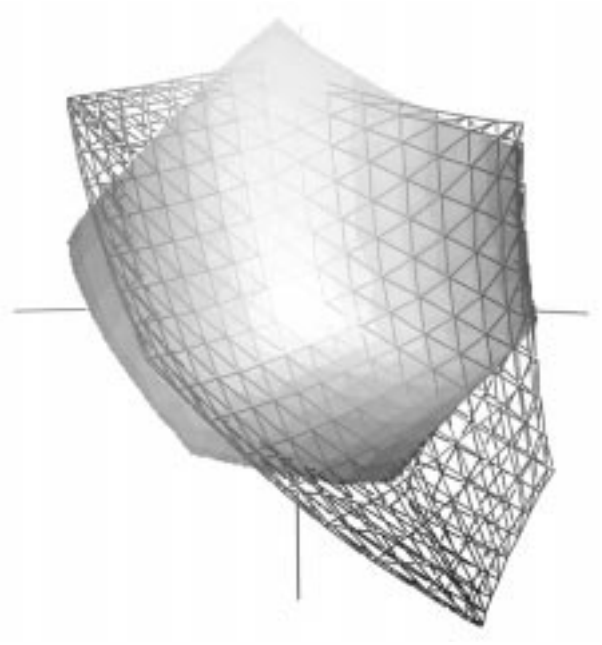

(a)

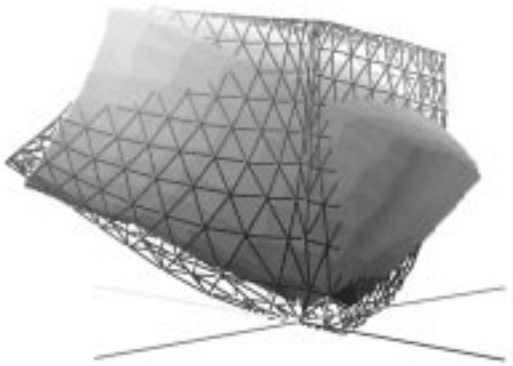

(b)

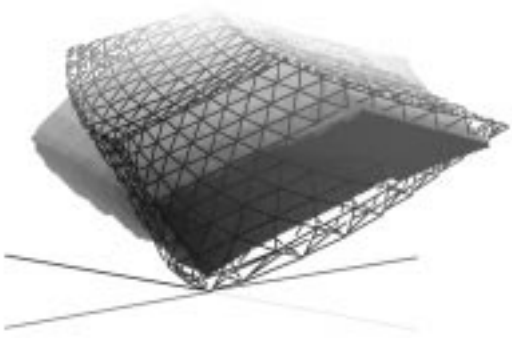

(c)

Fig. 5. Comparison of a CRT monitor gamut (shown as a wire frame) and a continuous-tone dye-sublimation printer gamut (shown as a solid) in CIELAB space. (a) Top view along the L^* axis. (b) and (c) Perspective projections.

1) CRT Displays: The most widely used display device for television and computer monitors is the color CRT. The face of a CRT is coated with a mosaic of red, green, and blue light emitting phosphors. The intensity of light emitted at each phosphor site is controlled by electrons striking it from an electron gun. Images are displayed by spatially modulating the RGB electron guns in accordance with the image signal. Since the mosaic is extremely fine, the eye

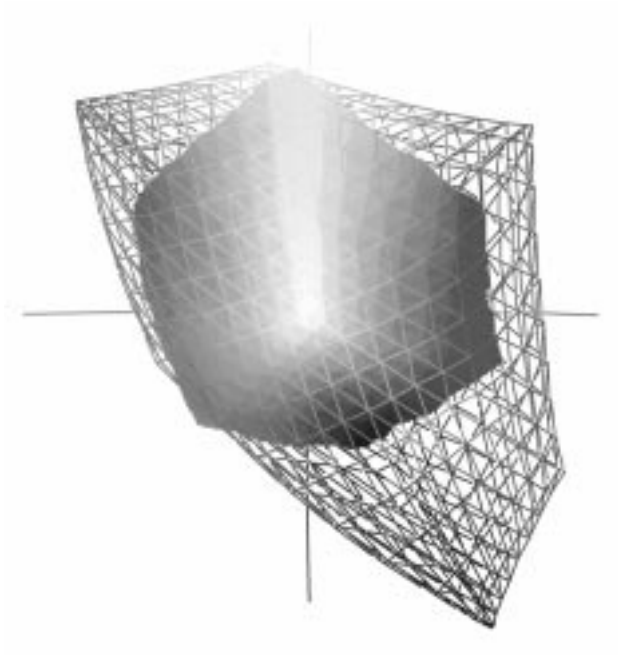

(a)

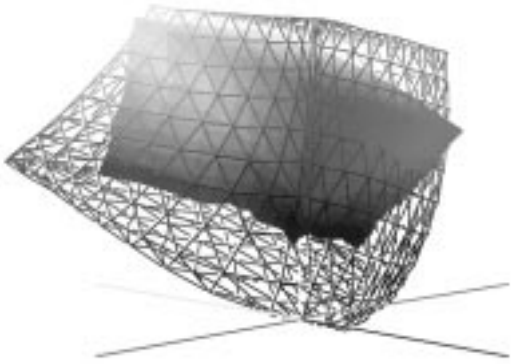

(b)

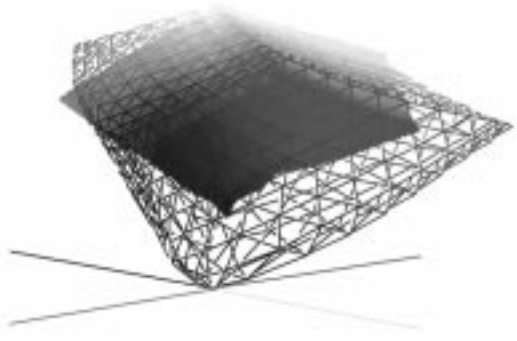

(c)

Fig. 6. Comparison of a CRT monitor gamut (shown as a wire frame) and an inkjet printer gamut (shown as a solid) in CIELAB space. (a) Top view along the L^* axis. (b) and (c) Perspective projections.

does not see the color of the individual phosphor sites but only a spatial average of the light from the individual red, green, and blue phosphors in a small region. The CRT is thus an additive color system.

The light emitted by each phosphor has a constant spectral composition independent of the driving voltages for the electron guns, except for an intensity scale factor. The scale factor is a nonlinear function of the driving voltage. A

typical model for the radiant spectrum emitted by a CRT is

$$s(\lambda) = \left(v_r/v_{m_r}\right)^{\gamma_r} s_r(\lambda) + \left(v_g/v_{m_g}\right)^{\gamma_g} s_g(\lambda) + \left(v_b/v_{m_b}\right)^{\gamma_b} s_b(\lambda) \quad (5)$$

where $s_r(\lambda)$ is the emission spectrum of the red CRT phosphor, v_r is the voltage applied to its associated electron gun, v_{m_r} is the maximum voltage for the red gun, and γ_r is the *monitor-gamma* for the red gun. The variables corresponding to the green and blue electron guns are defined similarly. The monitor-gamma is normally around 2.2 for most color monitors (for all three channels). Since the above parametric model is only approximate, several modifications of it have been used by researchers [35]–[38].

The CRT phosphors define a set of additive primaries. If the CMF's corresponding to these primaries are used in color specification, they can be directly used to drive the electron guns, provided the signals are precorrected for the power-law nonlinearity mentioned above. Typically, this is done in TV transmission. Since the operation involves exponentiation to the power of $1/\gamma$, it is known as *gamma correction*. A similar operation can also be done for digital-image data to be displayed on a computer CRT display. The quantization of gamma-corrected RGB tristimuli results in wider quantization intervals at higher amplitudes where the sensitivity of the eye is also lower. Therefore, just like speech companding, gamma correction of color tristimuli prior to quantization in a digital system (or transmission in a limited bandwidth system) reduces the perceptibility of errors and contours in comparison to a scheme in which no gamma correction is used [39], [40].

2) Color Printers: Unlike CRT's, which emit their own light, color printers produce images on paper (or transparency) for viewing under an external source of light. Color printers can be classified into two types: 1) *continuous-tone* (contone) printers and 2) halftone printers. Both contone and halftone printers produce color images by covering the paper with cyan, magenta, and yellow colorants that absorb light (largely) in the red, green, and blue spectral regions, respectively, and (commonly) a black colorant that absorbs light uniformly over the visible spectrum.

Contone printers are subtractive color devices. They use different concentrations of the cyan, magenta, and yellow colorants to control the absorption in the red, green, and blue regions and thereby produce different colors. A simple model of the subtractive process represents the spectrum of reflected light from a contone print as [1], [41]

$$g(\lambda) = l(\lambda) r_p(\lambda) 10^{-\sum_{i=1}^{4} c_i d_i(\lambda)} \quad (6)$$

where $l(\lambda)$ is the viewing illuminant spectrum, $r_p(\lambda)$ is the paper reflectance, $\{c_i\}_{i=1}^4$ are the concentrations of the colorants (normalized with respect to the maximum), and $\{d_i(\lambda)\}_{i=1}^4$ are their optical densities corresponding to the maximum concentrations. The digital values used to drive the printer determine the concentrations $\{c_i\}_{i=1}^4$ and thereby produce different colors.

Ideally, if one had CMY colorants that absorbed light in nonoverlapping regions of the spectrum and no black colorant, the above system of equations could be simplified and linearized. Actual physical colorants, however, have significant "unwanted absorptions" resulting in significant overlap. In addition, due to nonlinear interactions between the colorants in the printing process, (6) is often useful only as a qualitative model of the printing process. The same model (without the black colorant) is also used to represent both prints and slides from color photography.

Contone printers are rather sophisticated and expensive devices. Halftone color printers offer a significantly less expensive alternative with somewhat lower image quality. These printers produce color images by placing *halftone dots* composed of the CMYK colorants on paper. The colorants combine subtractively over the regions over which they overlap, resulting in a mosaic of differently colored regions on paper. Due to the low-pass nature of the eye's spatial response, the effective spectrum seen by the eye is the average of the spectra over a small angular subtense. Different colors are produced by varying the relative areas of the CMYK halftone dots, and the concentrations of the colorants within a dot are not varied. Since the overlapping of colorant dots is subtractive and the averaging over the spatial mosaic is additive, halftoning is a hybrid process.

A model for halftone printers was first suggested by Neugebauer [42], who observed that the overlap of CMY colorant halftone dots produces eight primary colors, which are now known as *Neugebauer primaries*. These include the paper (no ink), each of the three colorants (cyan, magenta, and yellow), combinations of two colorants (red, green-blue), and combinations of all three (black). Neugebauer proposed that the tristimulus values of the print can be expressed as the weighted average of the tristimuli of the Neugebauer primaries with the weights equal to their fractional area coverages. The model can readily be generalized from the three-colorant case to the case of four or any arbitrary number of colorants. Due to the penetration and scattering of light in paper, known as the *Yule–Nielsen effect* (or alternately as the optical dot gain) [43], [44], the simple Neugebauer model does not perform well in practice. As a result, several empirical modifications have been suggested for the model [45]. Recently, considerable success has been demonstrated in using a spectral version of the Neugebauer model with empirical corrections for the Yule–Nielsen effect [46]–[48], in which the reflectance of a CMYK halftone print is modeled as

$$r(\lambda; \mathbf{w}) = \left(\sum_{i=1}^{16} w_i {r_i}^{1/n}(\lambda) \right)^n \quad (7)$$

where $r_i(\lambda)$ and w_i are, respectively, the spectral reflectance and the fractional area of the ith primary (there are 16 primaries for a four-colorant (CMYK) system) and n is the empirical Yule–Nielsen correction factor.

Normally, the fractional areas w_i are themselves related to the fractional areas c, m, y, and k covered by the cyan, magenta, yellow, and black colorants, respectively.

The relations determining the w_i from c, m, y, and k depend on the method used to generate the halftone images. Equations for these relations were first derived by Demichel [49] by assuming independent random coverage for the colorants. Rotated halftone screens [50] that approximate this random independent coverage assumption are often used for printing because they are robust to commonly occurring registration (alignment) errors between the different colorants' images (*separations*). Alternate halftone screens have different characteristics and consequently different relationships between the fractional colorant coverages and the primary areas [51], [52].

B. Image Characteristics

The spectral radiance or reflectance of an image carries the most complete color information. Most color spectra are fairly smooth, and a 10-nm wavelength sampling is normally sufficient for representing these spectra [53]. The spectra of fluorescent gas-discharge lamps have sharp spectral peaks and therefore require a higher sampling rate or alternate model-based approaches [54]–[56]. A 10-nm sampling of spectra in the 400–700-nm region provides $N = 31$ samples[3] for each spectrum. Thus, color spectra lie in a 31-dimensional vector space. Color spectra are usually smooth, and therefore, they do not really exhibit 31 degrees of freedom. A principal-components analysis of common reflectance spectra reveals that a large fraction of the energy in these spectra is contained in a few principal components [57]. Several researchers have investigated this problem and have estimated that color-reflectance spectra can be represented by using anywhere between four and 12 principal components depending on the accuracy desired [58]–[61].

The spectral-reflectance characteristics discussed in the last paragraph covered almost the entire range of naturally occurring reflective objects.[4] Since most color-reproduction systems exploit trichromacy and have only three additive/subtractive primaries, their spectra often have even fewer degrees of freedom. Thus, the spectra from a CRT display lie in a 3-D space defined by the spectra of the phosphor primaries. The same is true of all additive systems that utilize three primaries. For subtractive and hybrid systems, though, there are often only three primaries; they are not confined to a 3-D space due to the nonlinearities in the subtractive process. For hybrid systems, the Neugebauer primaries may be viewed as additive primaries, but typically, the spectra of CMYK prints have fewer significant principal components than the 16 primaries in (7).

[3]The 400–700-nm interval is chosen for illustration, and the exact interval is not central to the argument here. Typical color-measurement instruments report spectra over this or a larger wavelength region.

[4]The color spectra of some naturally occurring objects arise from interference phenomena, which yield nonsmooth spectra that are not represented well by the principal components approach. Examples of such spectra are colors produced due to multiple film interference in certain minerals and iridescent colors on some bird feathers and in shells containing calcium carbonate [62, pp. 261, 267].

C. Computer-Generated Imagery

The last section focused on natural image scenes and *hard-copy* prints of these images. In the areas of multimedia applications, the computer is an alternate, rapidly growing source of color images. Computer-generated scenes and animations are now common in video games and movies [63], [64]. These applications strive for realistic images and therefore have to model the interactions between the lights and the objects in the scene using both geometric optics and colorimetry to produce proper color, shading, and texture for the surfaces involved [65, ch. 14]. For these applications to be successful in multimedia applications, it is necessary that the color information be recorded in a form that permits accurate rendering of the image on multiple output devices. This is particularly relevant in recording on movie film, which has entirely different characteristics from the CRT [66].

Color can also be used to effectively encode information for presentation and visualization. Bar graphs and pie charts used in presentations are simple examples of the use of colors to distinguish different regions. The capabilities of color encoding are also exploited more fully in applications that use color to represent quantitative differences in the data meaningfully. Examples of such applications include visualization of multispectral/stereo data using *pseudo-color* images and use of color to portray 3-D relationships in multidimensional data bases. The proper use of color in these and other multimedia applications greatly enhances their effectiveness [65, p. 601], [67]. Usually, the color images are designed for viewing on a CRT monitor and tend to exploit the full capabilities of the monitor. When printing these images, it is necessary to preserve their information and effectiveness. This is often a significant challenge because the printer gamuts are significantly smaller than monitor gamuts. Some of these problems and attempted solutions will be mentioned in Section IV-D.

D. Image-Recording Systems

Though the spectral radiance/reflectance carries the most complete color information for an image, it is usually both expensive and unnecessary to record this complete information. Instead, typical color-recording devices employ only three channels and exploit trichromacy of the eye or the characteristics of the original image medium to obtain color information.

Photography was the first widely available system for recording color images. Color photographs and slides are still one of the primary input sources for digital-imaging systems. Color photography film contains three light-sensitive emulsion layers that are exposed by the red, green, and blue spectral components of the incoming light. Through a process of development and printing, color images are produced by using cyan, magenta, and yellow colored dyes in accordance with the subtractive principles discussed earlier. Due to inherent nonlinearities and limitations in the chemical processes involved, exact colorimetric reproduction is difficult in photography.

In addition, due to the adaptation of the eye, exact colorimetric matches are also not desirable. Therefore, color photography normally attempts *preferred color reproduction* instead of accurate colorimetry [68, p. 191]. Since the original scene is rarely available for side-by-side comparison, this usually produces color images that are acceptable.

In digital color cameras, the film is replaced by an array of light-sensing charge-coupled-device (CCD) elements placed in 2-D arrays. The analog output from the light-sensing elements is quantized to obtain a digital image. Different schemes may be used to achieve the spatial-sampling and color-filtering operations concurrently. One arrangement uses three CCD arrays with red, green, and blue color filters, respectively. In such an arrangement, precise mechanical and optical alignment is necessary to maintain spatial correspondence between the images from the different color channels. For economy and in order to avoid the problems of registering multiple images, another arrangement, commonly referred to as a *color filter array* (CFA), uses a color filter mosaic, which is overlaid on the CCD array during the semiconductor processing steps. Since the green region of the spectrum is perceptually more significant, such mosaics are laid out so as to have green, red, and blue recording pixels in the ratio $2:1:1$ or $3:1:1$ [69], [70]. Image-restoration techniques are then used to reconstruct the full images for each of the channels [71], [72].

For recording color images that are available as prints, slides, negatives, or transparencies, color scanners are used. These devices operate on principles identical to those of the digital cameras except that they include an illuminant for use in the scanning process. The most common design uses an array of three linear CCD sensors with red, green, and blue color filters. The linear array covers one dimension of the scanned image and is scanned across in the other direction to obtain a complete image record. Since color slides and negatives have a very high spatial resolution and dynamic range in comparison with color prints, scanners for scanning these media are designed with high spatial sampling rates and large dynamic range. Also, these devices are often designed not for direct colorimetry (see Section III-D1) but for determining the densities of the cyan, magenta, and yellow colorants in the original. Thus, they employ color filters with narrow transmittance bands centered around the absorptance peaks of the colorants. A change in the colorants can therefore produce significant changes in the device's response, resulting in poor color recording unless the device is recalibrated for the new colorants. This is a significant problem since the colorants from different manufacturers vary significantly.

Cameras for capturing video images record a number of image frames per second. These are then displayed in succession on the display device to reconstruct the temporally varying scene. As far as color recording goes, these devices also typically employ three red, green, and blue channels and are not very different from digital cameras. Older designs use analog electronics that obtained the 2-D image by scanning the image over a raster of scan lines. In recordings for television, the raster lines are interlaced [73]. While this approach works fine for displaying video, usually restoration schemes are required to obtain still images for printing/display [74].

It is necessary to recognize that three channels are not sufficient for rendition of a natural reflectance scene under multiple viewing illuminants, and therefore additional channels should be used if modification of viewing conditions or scene parameters is anticipated. Recently, researchers have developed hyperspectral cameras that capture many image channels [75]. Currently, these devices are experimental and have been used in color-constancy research [76] and in simulation of digital cameras [77].

1) Requirements for Accurate Color Recording: The color-recording process in digital cameras, scanners, and video cameras can be represented by very similar mathematical models. In a manner analogous to (1), the output from these devices in response to a radiant spectrum $\mathbf{f}$ can be represented as $\mathbf{t}_s = \mathbf{M}_s^T \mathbf{f} + \boldsymbol{\epsilon}$, where $\mathbf{t}_s$ is the vector of measurements from the device, $\mathbf{M}$ is the $N\times 3$ matrix of spectral sensitivities of the (usually three) device channels, and $\boldsymbol{\epsilon}$ is the measurement noise [1].

From this model, it can be readily inferred that in the absence of noise, exact CIE XYZ tristimulus values can be obtained from the data recorded by the device if there exists a transformation that transforms the sensor response matrix $\mathbf{M}_s$ into the matrix of CIE XYZ color-matching functions, $\mathbf{A}$ [41]. For devices using three channels, this reduces to the requirement that $\mathbf{M}$ be a nonsingular linear transformation of $\mathbf{A}$. This fact has been known for some time and is referred to as the Luther–Ives condition [78], [79]. Recent reiterations of this result can be found in [80] and [81]. A device that satisfies (generalizations of) the Luther–Ives condition will be said to be *colorimetric*.

Due to practical design constraints, the Luther–Ives condition is rarely satisfied in practical devices. Besides, in the presence of noise, the condition does not necessarily imply optimality [82], and devices satisfying this condition can provide colorimetric information only under a single viewing illuminant. Consequently, several researchers have proposed measures for evaluating the sensitivities of a color-recording device. The first such measure was proposed by Neugebauer [83]. For a single filter, Neugebauer's quality factor measures the degree to which it is a linear transformation of the CMF's. Vora and Trussell [6], [84] extended the measure to an arbitrary number of device channels and viewing illuminants. A more comprehensive figure of merit that accounts for both the device noise and the nonlinearities in the color-perception process was proposed in [85]. This work also gave a unified framework for all these measures and work by other researchers in designing color filters that did not explicitly use a quality measure [86], [87].

It may be emphasized here that for a rendition of the recorded reflectance scene under multiple viewing illuminants, more than three channels are usually necessary. A simple generalization of the Luther–Ives condition would

require $3K$ channels for K different viewing illuminants. In practice, however, between four and seven optimally designed spectral channels provide sufficient accuracy for common viewing illuminants [86], [88].

Note that in recording color images digitally, both the spectrum and the spatial dimensions need to be "sampled." The different quality measures mentioned above consider only the spectral sampling aspect of the above problem. These are therefore suitable for evaluating the color-recording fidelity for large patches of uniform color and do not represent the complete performance for the image-recording system. This is particularly true in CFA camera devices, where the spatial and spectral sampling are performed jointly.

E. Quantization and Coding

Color images recorded with the different input devices described in the last section need to be quantized for digital processing. Both scalar- and vector-quantization techniques can be used in the quantization of color data. For simplicity, most color devices do independent quantization of the RGB channels with 8–12 bits per channel, with either uniform quantizers or companded quantizers that perform a gamma correction before the quantization. As mentioned earlier, the gamma correction significantly reduces the perceptibility of quantization errors, particularly in the 8-bit devices. For computer color displays based on a frame-buffer architecture [89], often only 8, 12, or 16 bits of video memory are allocated to each pixel, thereby allowing simultaneous display of only 2^8, 2^{12}, or 2^{16} colors, respectively. Vector-quantization techniques have therefore been extensively used for displaying images on these devices. A brief survey of some of these methods can be found in [1].

With the proliferation of digital color imagery, the problem of coding color images for transmission and storage has gained increased importance. It was recognized early on that the highly correlated RGB spaces were not suitable for independent coding [90]. Consequently, most of the methods transform the data into a luminance channel, and two chrominance channels that are then coded independently. A luminance chrominance space also allows coding schemes to exploit the properties of human vision by allocating significantly less bits to the high-frequency chrominance components, which are perceptually less significant.

The most prevalent compression scheme at present is the Joint Photographic Experts Group standard for still images [91] and the Moving Picture Experts Group standard for video data [92]. These standards are both based on the discrete cosine transform [93]. While these standards do not explicitly specify the color spaces to be used, in current implementations, it is common to use the YCrCb space [94], with the Cr and Cb components subsampled by a factor of two along both spatial dimensions [95]. The YCrCb color space is a luminance chrominance color space based on gamma-corrected RGB that has been proposed for use as a standard in high-definition TV. The Y component is a luminance channel similar to L^*, and the Cr and Cb are opponent chrominance channels similar to a^* and b^*, respectively.

F. Device Color Spaces

The measurements from color-recording devices and the control values for color-output devices are the color representations of recorded images or the images to be reproduced, respectively. Hence, it is common to say that these values represent colors in the device's color space. Thus, typically, there are RGB color spaces for scanners, cameras, and other input devices, and there are CMY/CMYK color spaces for color printers. Unlike the CIE and other color spaces mentioned in Section II-A, most of these color spaces are not standard and cannot be directly used for the meaningful archival/communication of image data. However, if these device spaces are related to the standard color spaces in a clear, unambiguous way, these can also be potentially used for the exchange of color information. An advantage of such a scheme is that no transformations of the image data are required for display if the data are specified in the native color space of the device. Since a large fraction of the images on the World Wide Web are primarily targeted for display on CRT monitors that have very similar characteristics, a new standard color space, sRGB, has been proposed for use based on these characteristics [96]. The sRGB color space is basically a gamma-corrected tristimulus space that uses the CRT phosphors as primaries for determining the CMF's. In addition, the sRGB standard includes provisions for specifying the viewing conditions (white-point chromaticities, image surround, flare, etc.).

IV. Color Management and Calibration

For proper color reproduction, the input and output devices involved need to be calibrated. Historically, the systems used for color reproduction were calibrated in a closed-loop configuration. As shown in Fig. 7, in a closed-loop configuration, the complete system is calibrated from input through output. Thus, for color photography, the film sensitivities, dye absorptances, and developmental interactions were appropriately chosen so as to result in acceptable reproduction. In offset printing, the scanner was used to generate CMYK "separations" that were suitable for generating halftone prints. With the increased use of digital computers and the evolution of desktop printing, it became obvious that such an approach has severe limitations. In particular, as the number of devices increases, calibrations for each input-output device pair are difficult to construct and maintain. In addition, since the calibrated data in a closed-loop calibration scheme is specific to one output device, it is not suitable for archival or exchange with devices outside the system.

With the growth of networking and increased exchange of color-image data between geographically divided systems, it was recognized that several of these problems can be solved by calibrating each device to a standard device-independent (DVI) color space, which can then be used for the exchange of data between different devices and for

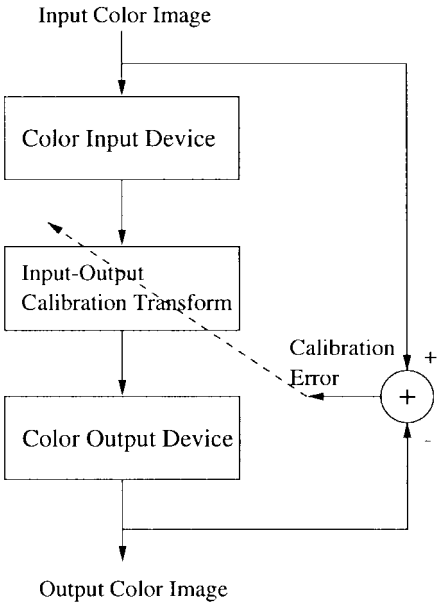

Fig. 7. Closed-loop system calibration.

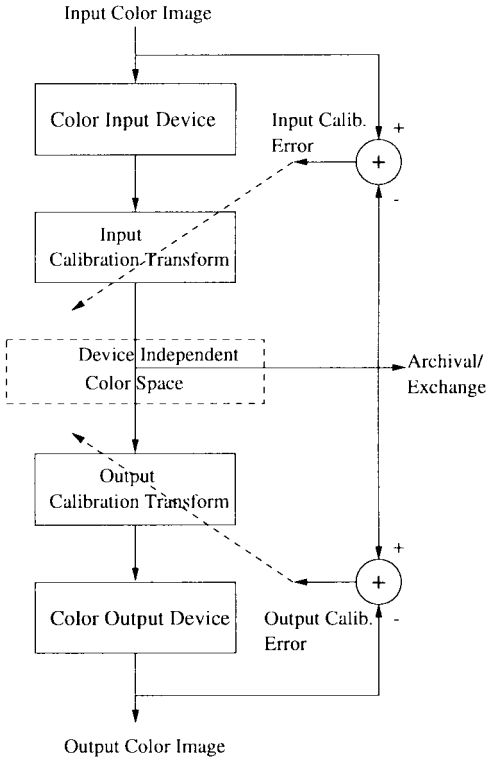

Fig. 8. Device-independent color calibration.

archival. As shown in Fig. 8, in these systems, the data from an input device are converted to a device-independent color space and then transformed into the device space of the target device for reproduction.

To enable proper management of color, several components are required. Color-measurement instrumentation is necessary for calibrating input and output systems. Standard formats for the storage and communication of these device calibrations are required so that different applications can make use of the calibrations. Also necessary are systems and algorithms that use the calibrations effectively to achieve desired results. These components are the subject of the remainder of this section.

A. Color-Measurement Instrumentation

A number of devices are available for the measurement of color. The correct instrument for a particular application depends on several factors, including the cost of the instrument, the accuracy desired, the variety of viewing conditions for which a calibration is desired, and the number and type of devices that need to be calibrated.

1) Spectroradiometers: A *spectroradiometer* is a device that measures the power of optical radiation as a function of wavelength. The measured spectrum provides the most complete description of color from which color descriptors in different color spaces can readily be computed. Most spectroradiometers contain an optical grating and a linear CCD array. Typical devices used for colorimetric work report data from about 380 to 780 nm at increments ranging from 2 to 10 nm. For most color work (including that using fluorescent lamps as sources), 2-nm sampling is sufficient [53]. Spectroradiometers can be used to measure both self-luminous and reflective objects. For the measurement of reflectance spectra, a spectrally smooth (preferably white) light source and a spectrally referenced sample (preferably white) are required. A comparison measurement between the known sample and the sample under question is made under identical conditions, allowing the determination of the unknown sample's reflectance spectrum, from which the color descriptor under any viewing illuminant can be obtained. Normally, the exact spectrum of the illuminant used with the spectroradiometer in the reflectance measurement is immaterial, provided it has sufficient power over the spectral range of interest. However, for the measurement of fluorescent materials, the power in the ultraviolet regions is also important, and the illuminant must closely approximate the desired standard illuminant under which colors are to be computed [97].

While spectroradiometers can measure both luminous and nonluminous objects, they are expensive, larger and less portable than the other instruments, and generally more difficult to operate due to their multiple operating modes. In particular, it can be difficult to set up a spectroradiometer for measuring reflectance samples under controlled conditions. There are automated systems for performing measurements on multiple samples using an x-y stage and a single light source.

2) Spectrophotometers: A *spectrophotometer* is a device for measuring the spectral reflectance of an object. Unlike a spectroradiometer, a spectrophotometer does not measure self-luminous objects. Therefore, spectrophotometers are useful for the calibration of printers and scanners but not of CRT displays. Spectrophotometers have their own internal light source, which illuminates the sample under measurement. There are many geometries for the sensor/illuminant combination, and each may be optimal for different applications. For publishing applications, the sensor and illuminant in the device are often set up for a 45°/0° condition,

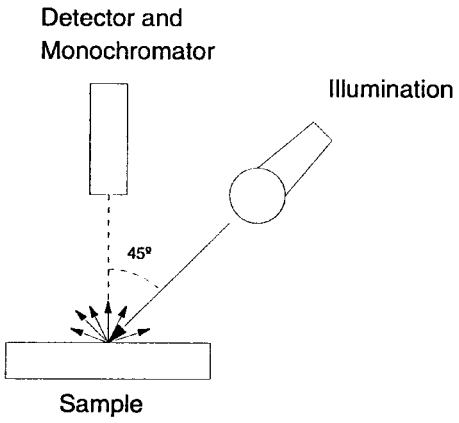

Fig. 9. 45°/0° measurement geometry.

as shown in Fig. 9. There are devices that illuminate the sample diffusely and measure off axis, allowing an option to include or exclude the specular component from the sample. Some devices contain an optical grating; others contain a filter wheel; and yet others use spectrally different light sources to illuminate the sample. Most devices report data from about 380 to 730 nm in 10–20-nm increments. Since reflectances of natural objects are smooth functions of wavelength and have low dimensionality, as discussed in Section III-B, these sampling rates are almost always sufficient [53].

Spectrophotometers measure reflectance as the ratio of two (uncalibrated) spectroradiometric measurements [1], [97] using the same principle that was described in the last section. They therefore come with a standard sample reflector, which is used to periodically recalibrate the instrument. Modern spectrophotometers are handheld, self-contained, and easy to operate. Some include automated stages for measuring multiple samples on a page. A disadvantage of most spectrophotometers is their cost, which, while less than that of a spectroradiometer, can often be prohibitive. The devices are also fragile, especially those with optical gratings or filter wheels.

3) Colorimeters and Photometers: As suggested by its name, a *colorimeter* measures color tristimuli and reports these as color values in CIE XYZ, CIELAB, or related color spaces. Some colorimeters have an internal light source for the measurement of color of reflective objects, while others measure only self-luminous or externally illuminated objects. For some devices, tristimulus values for the sample under a few different illuminants are available. Most colorimeters are small handheld devices with no moving parts, and they achieve their spectral separation by way of color filters or with spectrally different light sources. Colorimeters are less expensive than spectrophotometers and spectroradiometers, but they do not provide the detailed spectral information that allows the calibration of a printer for an arbitrary viewing illuminant. Those that measure self-luminous sources are used in the calibration of CRT's. *Photometers* are single-channel devices that provide a measurement of the luminance of a self-luminous or externally illuminated object. They are inexpensive and find use primarily in the calibration of CRT's when the chromaticity of the CRT phosphors is known.

B. Calibration and Profiles

Calibration of a color-imaging device relates its input/output to DVI color values. For an input device, calibration provides a mapping from device-measurement values (e.g., scanner RGB) to DVI color descriptors (e.g., CIE XYZ, CIELAB, etc.). For an output device, the calibration process yields a mapping from DVI color descriptors to device control values (e.g., CMYK, monitor RGB), which produce those color descriptors.

1) Input-Device Calibration: To calibrate a scanner, the first step is to select a collection of color patches that span the gamut of interest. Ideally, these colors should not be *metameric* for the scanner or the eye (under the illuminant for which the calibration is being produced). Metamerism is defined as the property in which different spectra map to the same values under a set of sensitivity functions. These patches are measured using a color-measurement instrument, such as a spectrophotometer or a colorimeter, which will provide the DVI color values $\{\mathbf{t}_k\}_{k=1}^{M_q}$, where M_q denotes the number of patches. Any of the (DVI) color spaces such as CIE XYZ, CIELAB, etc. can be used for this purpose. The use of CIELAB is common since this space includes information on the viewing illuminant in the white point. The patches are also measured with the scanner to obtain the scanner measurements $\{\mathbf{u}_k\}_{k=1}^{M_q}$.

To determine the CIE values for an arbitrary measured patch, the collected data are used to construct an interpolating function, which maps from the space of scanner-measurement values to the chosen DVI color space. This function, $F(\cdot)$, can then be used to relate any of the scanner RGB values to colorimetric XYZ values or LAB values, i.e., $F(\mathbf{u}) = \mathbf{t}$. Normally, a parametric form is chosen for $F(\cdot)$, and the parameters are determined through regression. Several different schemes have been used for this purpose, ranging from straightforward linear and polynomial regression to neural networks [98, ch. 11]. Usually, $F(\cdot)$ is complicated and computationally expensive. For this reason, usually $F(\cdot)$ is used to produce a finely sampled lookup table (LUT) from which $F(\cdot)$ at arbitrary points is obtained by using simple interpolation schemes [98, ch. 4].

Calibration for digital cameras and video cameras is usually done in a similar fashion by using a target of patches with known reflectances or color values. Since the eye is very sensitive to deviations from the neutral (achromatic) colors, sometimes an additional one-dimensional (1-D) transform is included on each of the RGB channels so that the $R = G = B$ line corresponds to neutral colors. This procedure is commonly referred to as *gray/white balancing*.

2) Output-Device Calibration: For calibrating an output device, a transformation from DVI color values to the space of device control values is required. This requires a two-step procedure. In the first step, the printer characterization, which determines the forward transformation from printer

control values to DVI color values, is determined. Then, this forward transform is used in the next step to determine the inverse mapping from DVI color values to device control values.

Since CRT monitors are represented well by the parametric models described in Section III-A1, the forward characterization of these devices is usually done by determining the model parameters from a few measurements. It can also be readily seen that due to their additive nature, the inverse transformation from CIE XYZ (or other tristimulus) values to the CRT control voltages can be computed by means of a simple matrix transformation followed by a 1-D transform for the gamma correction. This scheme is used in all cases, except those requiring the highest accuracy, for which LUT-based schemes may be used and additional corrections may be made for the surface reflection (flare) from the monitor screen. In addition, it may be necessary to correct for the significant spatial nonuniformity over the CRT screen [1], [99].

For the forward characterization of printers, commonly an empirical scheme similar to that described for scanner calibration is used. By selecting a set of printer control values $\{\mathbf{c}_k\}_{k=1}^{M_p}$ covering the range of allowable control values, measuring the corresponding DVI color values $\{\mathbf{v}_k\}_{k=1}^{M_p}$, and using some interpolation scheme, the forward mapping $\mathbf{v} = G(\mathbf{c})$ from control values to DVI color values is determined. For halftone printers, alternately, the Neugebauer models mentioned in Section III-A2 have also been used. Since even the models are nonlinear and not readily invertible, for the inverse mapping $G^{-1}(\cdot)$, invariably an interpolating function is used to get a finely sampled LUT. Due to the four degrees of freedom in the control values of CMYK printers, there exist multiple control values that result in the same printed color. Since this poses a challenge in obtaining a smooth inverse mapping, often the inverse determines the amounts of three virtual CMY colorants, from which the CMYK control values are obtained by some functional relation. This process is viewed as the incorporation of black ink and removal of underlying CMY inks and is commonly referred to as *undercolor removal* (UCR). Typically, the UCR mapping from the virtual CMY values to actual CMYK control values is designed so as to render achromatic colors better, reduce total colorant amounts (for faster drying/better adhesion to paper), and (in some cases) reduce the use of the expensive CMY colorants.

3) Device Profiles: To make the calibration transformations available to different applications that wish to use them, the calibration transformation for each device is stored in a device profile. In the early days of color management, different manufacturers used their own proprietary formats for the storage of these profiles, which were therefore useful only for applications from the same manufacturer. To realize the full benefits from the DVI calibration of devices, the desktop-publishing industry is increasingly moving toward open systems. A standard format for the storage of device profiles has been defined and is being widely adopted [100]. This International Color Consortium profile format specifies a wide variety of input and output device profiles suitable for efficiently representing the color-calibration information. The use of a standardized format allows the profiles to be used by different applications from different manufacturers.

C. Color-Management Systems (CMS's)

A CMS is responsible for interpreting the device profiles and performing the appropriate transformations to/from the DVI space. The goal of a CMS is to provide predictable and consistent color without requiring specialized skills from the user. Thus CMS's tie together device profiles with *color-matching modules* that use these device profiles to transform device-dependent image data to DVI color spaces or to the device color spaces of target output devices on which the images are to be displayed. In addition, the CMS provides the user with flexibility to choose different *rendering intents* for different images. Thus, for instance, in reproducing a company logo, a perfect colorimetric match is usually desired; in producing bar graphs and pie charts for presentation, it is desirable that the colors be highly saturated for maximal impact; and in reproducing pictorial images, it is desirable that the closest perceptual match be obtained (which will depend on viewing conditions). Color-management functions can be performed at several different phases of the imaging process: in the devices (e.g., Adobe Postscript level 2 for printers), in device drivers (e.g., Canon Colorgear), in applications (e.g., Adobe Photoshop), or in the operating system (e.g., Apple's ColorSync). The notion of embedding color management in the operating system has the potential of making the process transparent to the end user and is therefore gaining acceptance rapidly, with several vendors of operating systems for desktop and workstation computers incorporating CMS's into their products.

Ideally, with color management, one could accurately transfer color information from one medium (e.g., CRT) to another (e.g., print). Unfortunately, this is an extremely difficult task due to two reasons: 1) there are significant differences in gamuts of different devices (this was mentioned and demonstrated in Section III-A) and 2) the difference in typical viewing conditions for different media implies that a simple colorimetric match does not give an appearance match. There is therefore significant interest in *gamut-mapping* algorithms that map the colors in an image to suitable colors that can be reproduced on the target device. Methods that model the adaptations of the eye and allow the computation of appearance-matched images under different viewing conditions are also an active area of research.

D. Gamut Mapping

Gamut mapping is the process of mapping the displayable colors from one media to those of another media. As defined earlier, the ideal goal for color matching depends on the type of the image and the intent of the user. The problem is probably most acute for pictorial images for which ideally one would like to map the colors so as

to obtain the best possible appearance match between the images on the different media [101], [102]. The strategy for gamut mapping could be either image dependent or image independent. Since image-dependent methods can use different strategies for different images, they often produce better results. However, they are also significantly slower than image-independent techniques because they require a fresh computation for each image, and are therefore seldom used in automatic gamut-mapping schemes. Several color applications, however, indicate out-of-gamut colors in an image via a key color or a flashing highlight (on a CRT). This allows the user to perform a transformation such that these colors are mapped to his satisfaction. Such an approach, however, requires considerable operator skill in order to obtain satisfactory results.

The simplest technique of gamut mapping (particularly for CRT monitors) is clipping in the space of device control values. Since the space of control values is not a UCS, clipping of control values does not yield the closest printable color (as perceived by an observer). To remedy this problem, a simple extension would be to map out-of-gamut colors to the nearest in-gamut color in a UCS. While this approach offers significantly better results than the device space clipping [103], it can often result in unacceptable hue shifts that are perceptually very objectionable. An additional limitation of this and the clipping approach is that smoothly varying regions beyond the device gamut can potentially be mapped to a single color, creating undesirable abrupt edges in the previously smooth regions and causing loss of significant information (such as shape from shading).

Another approach used for gamut mapping is a gamut-compression algorithm, which compresses all the colors in the image in a manner that reduces the colorimetric dynamic range in the image while ensuring that the colors can be reproduced. For example, one could move all the colors in the image toward one point, such as a midgray, until all the colors in the image are within the device gamut. Unlike the clipping approach, this method will retain some of the variation in smoothly varying image regions that are beyond the device gamut. In addition to UCS's, notions of hue, chroma, and saturation/value are extremely useful in gamut-mapping research since these can be directly related to viewers' objections to artifacts produced by gamut-mapping algorithms and can be used in appropriately choosing the clipping and compression. In Section II-D1, it was pointed out that in addition to being a UCS, the CIELAB space allows the computation of correlates of lightness, hue, and chroma. As a result, CIELAB has been used extensively in gamut-mapping research. A recent comparison of a number of clipping- and compression-based gamut-mapping schemes in CIELAB space can be found in [104], [105].

The transformations to and from the perceptual spaces are usually nonlinear, and speed is often an issue [106]. For this reason, some CMS's may use a high-resolution LUT along with a linear interpolator to perform the transformation. Performing multiple transforms on the data can result in a loss of fidelity and introduce visually noticeable errors due to the accumulation of errors associated with finite precision arithmetic. Some CMS's can cache input and output transformations, concatenate these, and perform these in a single operation when the final image is desired. This not only saves time but also improves accuracy.

E. Appearance Matching

Section II-D briefly discussed the adaptation in the eye in response to changes in viewing conditions. Since different color-reproduction media have different viewing conditions, in reproducing images across these different media, an appearance match instead of a pure colorimetric match is usually desired. The simplest instance of appearance matching is the white-point matching method based on the Von Kries transformation, as mentioned in Section II-D1. This transformation converts tristimuli into a space of cone responses and applies a diagonal correction matrix that equates the white points under the two viewing conditions [7, p. 432]. White-point matching is often used in color-imaging applications, and there is support for it in several color-management applications and packages, such as Postscript.

In addition to white-point adaptation, there are several well-characterized psychophysical effects that change with changes in viewing conditions. In particular, it is well documented that the apparent contrast (perceived intensity gradient) of an image decreases in a dark surround in comparison to a bright surround [68, pp. 49–57]. Often, this change in contrast is modeled by relating the luminance to the perceived lightness as a power-law relation, similar to that for CIELAB in (3), with the exponent's increasing as the surround gets brighter [68, pp. 56–57], [107]. Thus, "gamma correction" has also been used extensively to compensate for these effects, in addition to correction for monitor nonlinearity.

There has been considerable research in defining color-appearance models that account for chromatic adaptation, influence of surround, and other psychophysical phenomena that affect the perception of images [24]. Comparative results of several different color-appearance models in imaging applications can be found in [24] and [108]. These models hold tremendous potential for use in cross-media color reproduction. The CIE is involved in an ongoing attempt to define a standard appearance model for use in imaging applications. An interim version of the model is available [109], which is expected to be subsequently refined.

V. Illustrative Example

This paper has reviewed the background of color science and color terminology, discussed the instrumentation, and discussed how to communicate color among various devices. Let us consider how to put all of these things together in an illustrative application. Rather than review in detail published applications that demonstrate a few parts of the color process, a fictitious but plausible application is

described that uses most of the concepts and tools discussed in the previous sections.

In both animation and simulation, the problem of changing lighting conditions arises. In the case of animation, the user specifies the lighting conditions and surface properties of the objects. The process that is addressed here is creating a new image from an original and reproducing it accurately on a different medium. We will assume a case with a single light source.

Since a single illumination is used, the radiant spectrum of every object can be represented by the model used in (2). It is not required that every object be represented by a 31-dimensional vector since, as mentioned previously, most reflective objects in the real world have many fewer degrees of freedom. To obtain accurate color under multiple illuminants, however, more than three dimensions are required. In any case, all of the vector equations and principles discussed earlier hold, regardless of dimensionality. The change in color for each pixel can be computed directly from the vector that describes the pixel without auxiliary computation, which requires geometrical considerations. In this case, the new color is given by

$$\mathbf{t} = \mathbf{A}^T \mathbf{L}_{\text{new}} \mathbf{r} \tag{8}$$

where $\mathbf{r}$ is the vector representing the reflective spectra of the pixel, $\mathbf{L}_{\text{new}}$ represents the new illumination [see (2)], $\mathbf{A}$ is the CMF, and $\mathbf{t}$ is the vector of new tristimulus values.

Let us assume that an image or sequence of images has been created that correspond to midday illumination. It is desired to render the scene as it would appear in the late afternoon. The data that describe the image, not the objects in the image, are the tristimulus values of each pixel. As is common, let us use CIELAB. Since the CIELAB values depend on a normalizing white point, this point must be specified for a complete definition of the image. In this case, the white point would correspond to the midday (approximately D6500) spectra of the assumed illuminant.

The image was designed using a computer and thus viewed on a CRT monitor. To use the monitor for evaluation, the monitor must be calibrated using the methods described in Section IV-B2. The image-lab values, along with the white point, are converted to monitor RGB values using the calibration. The transformation from lab to RGB may also require gamut mapping. The designer who created the original image should take into account the gamut of the devices that will be used. It is prudent to avoid out-of-gamut colors as much as possible. The designer would probably alter the colors, i.e., reflectances, of the objects to obtain the best visual effect.

The change of illuminant to late afternoon (approximately D2000) results in new lab values and a new white point. Recall that the white point is used as a compensation for the adaptive ability of the eye. An example of this adaptation is that white objects will appear white to the viewer under a wide range of illumination. Thus, despite the fact that the reflected spectrum from a white object in the afternoon would have a much higher red component than at midday, it will still appear white. However, the relative colors of other objects may shift. The tristimulus values can be computed via (8). However, note that to view the image correctly, the white point of the monitor should be changed to correspond to the new viewing conditions. To obtain the most accurate color transformation, more than three color bands of reflectance should be used to describe the reflectance of the pixel. If the color transformation is done from the three lab values, some error is inevitable. This error can be minimized by using a statistical description of the spectra of the objects in the image [110].

The designer is happy with the appearance of the image on the monitor. Now it is desired to print the image on film for display. Again, the process of color communication is started. The film will be projected so that the white point of the display is fixed by the lamp and screen combination. The pixel values are now transformed to exposure values, which control the density of the dyes on the film. Again, gamut mapping must be done. Since this is the final display for the design procedure, this is the gamut that should control the entire process.

VI. Summary

To use color in multimedia applications effectively, one needs to understand color from a perspective that goes beyond the simple RGB "color space" model often used in computer applications. This paper aims at explaining the issues involved in using calibrated and accurate color for multimedia applications. The basics of color science, management, and calibration are explained along with the challenges involved in reproducing images on a multiplicity of output devices. The use of the concepts is demonstrated through an illustrative example.

Acknowledgment

The authors wish to thank Dr. R. Balasubramanian for his helpful suggestions and pointers and J. Stinehour for making available the data used in Figs. 5 and 6.

References

[1] G. Sharma and H. J. Trussell, "Digital color imaging," *IEEE Trans. Image Processing*, vol. 6, pp. 901–932, July 1997.
[2] H. J. Trussell, "Application of set theoretic models to color systems," *Color Res. Appl.*, vol. 16, no. 1, pp. 31–41, Feb. 1991.
[3] B. K. P. Horn, "Exact reproduction of color images," *Comput. Vis., Graphics Image Process.*, vol. 26, pp. 135–167, 1984.
[4] J. B. Cohen, "Color and color mixture: Scalar and vector fundamentals," *Color Res. Appl.*, vol. 13, no. 1, pp. 5–39, Feb. 1988.
[5] H. J. Trussell and J. R. Sullivan, "A vector-space approach to color imaging systems," in *Proc. SPIE Image Processing Algorithms and Techniques*, K. S. Pennington, Ed., 1990, vol. 1244, pp. 264–271.
[6] P. L. Vora and H. J. Trussell, "Measure of goodness of a set of color scanning filters," *J. Opt. Soc. Amer. A*, vol. 10, no. 7, pp. 1499–1508, 1993.
[7] G. Wyszecki and W. S. Stiles, *Color Science: Concepts and Methods, Quantitative Data and Formulae*, 2nd ed. New York: Wiley, 1982.
[8] International Commission on Illumination, "Colorimetry," Central Bureau of the CIE, Vienna, Austria, CIE Pub. 15.2, 1986.
[9] H. S. Fairman, M. H. Brill, and H. Hemmendinger, "How the CIE 1931 color-matching functions were derived from Wright-

Guild data," *Color Res. Appl.*, vol. 22, no. 1, pp. 11–23, Feb. 1997.
[10] P. K. Kaiser and R. M. Boynton, *Human Color Vision*, 2nd ed. Washington, DC: Optical Society of America, 1996.
[11] National Television Systems Committee, "NTSC signal specifications," *Proc. IRE*, vol. 42, pp. 17–19, Jan. 1954.
[12] Society for Motion and Television Pictures, "Color temperature for color television studio monitors," SMPTE Recommended Practice RP 37-1969, White Plains, NY, July 1969.
[13] Society for Motion and Television Pictures, "Color monitor colorimetry," SMPTE recommended practice RP 145–1987, White Plains, NY, June 1987.
[14] B. A. Wandell, *Foundations of Vision*. Sunderland, MA: Sinauer Associates, 1995.
[15] C. S. McCamy, "Correlated color temperature as an explicit function of chromaticity coordinates," *Color Res. Appl.*, vol. 17, no. 2, pp. 142–144, Apr. 1992.
[16] R. W. G. Hunt, "The specification of color appearance. I. Concepts and terms," *Color Res. Appl.*, vol. 2, no. 2, pp. 55–68, Summer 1977.
[17] ——, "Color terminology," *Color Res. Appl.*, vol. 3, no. 2, pp. 79–87, Summer 1978.
[18] ——, *Measuring Color*, 2nd ed. New York: Ellis Horwood, 1991.
[19] E. Q. Adams, "A theory of color vision," *Psychol. Rev.*, vol. 36, pp. 56–76, 1923.
[20] M. Mahy, L. Van Eyckden, and A. Oosterlinck, "Evaluation of uniform color spaces developed after the adoption of CIELAB and CIELUV," *Color Res. Appl.*, vol. 19, no. 2, pp. 105–121, Apr. 1994.
[21] F. J. J. Clarke, R. McDonald, and B. Rigg, "Modification to the JPC79 color-difference formula," *J. Soc. Dyers Colorists*, vol. 100, pp. 128–132, 1984.
[22] International Commission on Illumination, "Industrial color difference evaluation," Central Bureau of the CIE, Vienna, CIE Pub. 116–1995, 1995.
[23] J. A. Von Kries, "Die Gesichtsempfindungen," in *Handbuch der Physiologie der Menschen, Tiel III*, W. Nagel, Ed., vol. 3. Brunswick: Vieweg, 1905, pp. 109–282.
[24] M. D. Fairchild, *Color Appearance Models*. Reading, MA: Addison-Wesley, 1998.
[25] D. H. Kelly, "Spatial and temporal interactions in color vision," *J. Imaging Tech.*, vol. 15, no. 2, pp. 82–89, Apr. 1989.
[26] E. Granger, "Uniform color space as a function of spatial frequency," in *Proc. IS&T 7th Int. Conf. Advances in Non-Impact Printing Technology*, 1991, pp. 309–322.
[27] X. Zhang and B. A. Wandell. (1996). Spatial extension of CIELAB for digital color image reproduction, *Proceedings of the SID International Conference*. [Online]. Available URL: http://white.stanford.edu:80/html/xmei/.
[28] W. Frei and B. Baxter, "Rate-distortion coding simulation for color images," *IEEE Trans. Commun.*, vol. COM-25, pp. 1385–1392, Nov. 1977.
[29] O. D. Faugeras, "Digital color image processing within the framework of a human visual model," *IEEE Trans. Acoust., Speech, Signal Processing*, vol. 27, pp. 380–393, Aug. 1979.
[30] S. Daly, "The visual differences predictor: An algorithm for the assessment of image fidelity," in *Digital Images and Human Vision*, A. B. Watson, Ed. Cambridge, MA: MIT Press, 1993, pp. 179–206.
[31] J. Lubin, "A visual discrimination model for imaging system design and evaluation," in *Vision Models for Target Detection and Recognition*, E. Peli, Ed. River Edge, NJ: World Scientific, 1995, pp. 245–283.
[32] G. Sharma, M. J. Vrhel, and H. J. Trussell. (1998). Color figures for this paper. [Online]. Available URL: http://www4.ncsu.edu/gsharma/public_html/color_multimedia/; http://www4.ncsu.edu/eos/users/h/hjt/WWW/index_figures.html.
[33] R. Rolleston, "Visualization of colorimetric calibration," in *Proc. SPIE Color Hard Copy and Graphic Arts II*, J. Bares, Ed., 1993, vol. 1912, pp. 299–309.
[34] D. Kalra, "GamOpt: A tool for visualization and optimization of gamuts," in *Proc. SPIE Color Hard Copy and Graphic Arts III*, J. Bares, Ed., 1994, vol. 2171, pp. 299–309.
[35] W. B. Cowan, "An inexpensive scheme for calibration of a color monitor in terms of standard CIE coordinates," *Comput. Graph.*, vol. 17, pp. 315–321, July 1983.
[36] R. S. Gentile, J. P. Allebach, and E. Walowit, "Quantization of color images based on uniform color spaces," *J. Imaging Technol.*, vol. 16, pp. 11–21, Feb. 1990.
[37] R. S. Berns, R. J. Motta, and M. E. Gorzynski, "CRT colorimetry, Part I: Theory and practice," *Color Res. Appl.*, vol. 18, no. 5, pp. 299–314, Oct. 1993.
[38] R. S. Berns, M. E. Gorzynski, and R. J. Motta, "CRT colorimetry, Part II: Metrology," *Color Res. Appl.*, vol. 18, no. 5, pp. 315–325, Oct. 1993.
[39] F. Kretz, "Subjectively optimal quantization of pictures," *IEEE Trans. Commun.*, vol. COM-23, pp. 1288–1292, Nov. 1975.
[40] C. A. Poynton, "'Gamma' and its disguises: The nonlinear mappings of intensity in perception, CRT's, film, and video," *SMPTE J.*, vol. 102, pp. 377–385, Dec. 1993.
[41] H. J. Trussell, "DSP solutions run the gamut for color systems," *IEEE Signal Processing Mag.*, vol. 10, pp. 8–23, Apr. 1993.
[42] H. E. J. Neugebauer, "Die Theoretischen Grundlagen des Mehrfarbenbuchdrucks," *Zeitschrift für Wissenschaftliche Photographie Photophysik und Photochemie*, vol. 36, no. 4, pp. 73–89, Apr. 1937.
[43] J. A. C. Yule and W. J. Neilsen, "The penetration of light into paper and its effect on halftone reproduction," in *Proc. TAGA*, May 7–9, 1951, pp. 65–76.
[44] F. R. Clapper and J. A. C. Yule, "Reproduction of color with halftone images," in *Proc. 7th Annual Tech. Meeting TAGA*, May 9, 1955, pp. 1–14.
[45] K. Sayangi, Ed., *Proceedings of the SPIE: Neugebauer Memorial Seminar on Color Reproduction*, Bellingham, WA, Dec. 14–15, 1989, vol. 1184.
[46] J. A. S. Viggiano, "Modeling the color of multi-colored halftones," *Proc. TAGA*, 1990, pp. 44–62.
[47] R. Rolleston and R. Balasubramanian, "Accuracy of various types of Neugebauer models," in *Proc. IS&T/SID Color Imaging Conf.: Transforms and Portability of Color*, Nov. 1993, pp. 32–37.
[48] R. Balasubramanian, "Colorimetric modeling of binary color printers," in *Proc. IEEE Int. Conf. Image Processing*, Nov. 1995, pp. II-327–330.
[49] E. Demichel, *Procédé*, vol. 26, pp. 17–21, 26–27, 1924.
[50] J. A. C Yule, *Principles of Color Reproduction, Applied to Photomechanical Reproduction, Color Photography, and the Ink, Paper, and Other Related Industries*. New York: Wiley, 1967.
[51] R. Balasubramanian, "A printer model for dot-on-dot halftone screens," in *Proc. SPIE Color Hard Copy and Graphic Arts IV*, J. Bares, Ed., 1995, vol. 2413, pp. 356–364.
[52] W. L. Rhodes and C. M. Hains, "The influence of halftone orientation on color gamut and registration sensitivity," in *Proc. IS&T's 46th Ann. Conf.*, May 1993, pp. 180–182.
[53] H. J. Trussell and M. S. Kulkarni, "Sampling and processing of color signals," *IEEE Trans. Image Processing*, vol. 5, pp. 677–681, Apr. 1996.
[54] D. L. MacAdam, *Color Measurement: Theme and Variations*, 2nd ed. New York: Springer-Verlag, 1981.
[55] H. J. Trussell and M. Kulkarni, "Estimation of color under fluorescent illuminants," in *Proc. IEEE Int. Conf. Image Processing*, 1994, pp. III1006–1010.
[56] G. Sharma and H. J. Trussell, "Decomposition of fluorescent illuminant spectra for accurate colorimetry," in *Proc. IEEE Int. Conf. Image Processing*, Nov. 1994, pp. II1002–1006.
[57] I. T. Jolliffe, *Principal Components Analysis*. Berlin, Germany: Springer-Verlag, 1986.
[58] J. Cohen, "Dependency of the spectral reflectance curves of the Munsell color chips," *Psychronomic Sci.*, vol. 1, pp. 369–370, 1964.
[59] L. T. Maloney, "Evaluation of linear models of surface reflectance reflectance with a small number of parameters," *J. Opt. Soc. Amer. A*, vol. 3, pp. 1673–1683, 1986.
[60] B. A. Wandell, "The synthesis and analysis of color images," *IEEE Trans. Pattern Anal. Machine Intell.*, vol. PAMI-9, pp. 2–13, Jan. 1987.
[61] M. J. Vrhel, R. Gershon, and L. S. Iwan, "Measurement and analysis of object reflectance spectra," *Color Res. Appl.*, vol. 19, no. 1, pp. 4–9, Feb. 1994.

[62] K. Nassau, *The Physics and Chemistry of Color: The Fifteen Causes of Color*. New York: Wiley, 1983.
[63] B. Robertson, "*Toy Story:* A triumph of animation," *Comput. Graph. World*, vol. 18, no. 8, pp. 28–38, Aug. 1995.
[64] D. Coco, "Breathing life into 3-d humans," *Comput. Graph. World*, vol. 18, no. 8, pp. 28–38, Aug. 1995.
[65] J. D. Foley, A. van Dam, and J. F. Hughes, *Computer Graphics: Principles and Practice*, 2nd ed. Reading, MA: Addison-Wesley, 1993.
[66] M. Kulkarni and M. Grant, "Color management and film recorders," *Photographic Process.*, pp. 52–53, Jan. 1995.
[67] R. Vetter, C. Ward, and S. Shapiro, "Using color and text in multimedia projections," *IEEE Multimedia Mag.*, vol. 2, pp. 46–54, Winter 1995.
[68] R. W. G. Hunt, *The Reproduction of Color in Photography, Printing, and Television*, 4th ed. Tolworth, England: Fountain Press, 1987.
[69] R. P. Khosla, "From photons to bits," *Phys. Today*, vol. 45, no. 12, pp. 42–49, Dec. 1992.
[70] K. A. Parulski, L. J. D'Luna, B. L. Benamati, and P. R. Shelley, "High-performance digital color video camera," *J. Electron. Imaging*, vol. 1, no. 1, pp. 35–45, Jan. 1992.
[71] D. H. Brainard, "Bayesian method for reconstructing color images from trichromatic samples," in *IS&T's 47th Ann. Conf., ICPS'94: Physics and Chemistry of Imaging Systems*, May 15–20, 1994, vol. 2, pp. 375–380.
[72] D. R. Cok, "Reconstruction of CCD images using template matching," in *IS&T's 47th Ann. Conf., ICPS'94: Physics and Chemistry of Imaging Systems*, May 15–20, 1994, vol. 2, pp. 380–385.
[73] K. B. Benson and J. C. Whitaker (Eds.), *Television Engineering Handbook: Featuring HDTV Systems*. New York: McGraw-Hill, 1992.
[74] A. J. Patti, M. I. Sezan, and A. M. Tekalp, "Robust methods for high-quality stills from interlaced video in the presence of dominant motion," *IEEE Trans. Circuits Syst. Video Technol.*, vol. 7, pp. 328–342, Apr. 1997.
[75] D. H. Brainard. (1997). Hyper-spectral image data. [Online]. Available WWW: http://color.psych.ucsb.edu/hyperspectral/.
[76] D. H. Brainard, W. A. Brunt, and J. M. Speigle, "Color constancy in the nearly natural image, 1. Asymmetric matches," *J. Opt. Soc. Amer. A*, vol. 14, no. 9, pp. 2091–2110, Sept. 1997.
[77] P. L. Vora, M. L. Harville, J. E. Farrell, J. D. Tietz, and D. H. Brainard, "Image capture: Synthesis of sensor responses from multispectral images," in *Proc. SPIE Color Imaging: Device Independent Color, Color Hard Copy, and Graphic Arts II*, 1997, vol. 3018, pp. 2–11. (Available URL: http://color.psych.ucsb.edu/hyperspectral/.)
[78] R. Luther, "Aus Dem Gebiet der Farbreizmetrik," *Z. Tech. Phys.*, vol. 8, pp. 540–558, 1927.
[79] H. E. Ives, "The transformation of color-mixture equations from one system to another," *J. Franklin Inst.*, vol. 16, pp. 673–701, 1915.
[80] P. C. Hung, "Colorimetric calibration for scanners and media," in *Proc. SPIE*, 1991, vol. 1448, pp. 164–174.
[81] J. J. Gordon and R. A. Holub, "On the use of linear transformations for scanner calibration," *Color Res. Appl.*, vol. 18, no. 3, pp. 218–219, June 1993.
[82] G. Sharma and H. J. Trussell, "Color scanner performance trade-offs," in J. Bares, Ed., *Proc. SPIE Color Imaging Device-Independent Color, Color Hard Copy, and Graphic Arts*, 1996, vol. 2658, pp. 270–278.
[83] H. E. J. Neugebauer, "Quality factor for filters whose spectral transmittances are different from color mixture curves, and its application to color photography," *J. Opt. Soc. Amer.*, vol. 46, no. 10, pp. 821–824, Oct. 1956.
[84] P. L. Vora and H. J. Trussell, "Mathematical methods for the design of color scanning filters," *IEEE Trans. Image Processing*, vol. 6, pp. 312–320, Feb. 1997.
[85] G. Sharma and H. J. Trussell, "Figures of merit for color scanners," *IEEE Trans. Image Processing*, vol. 6, no. 7, pp. 990–1001, July 1997.
[86] M. J. Vrhel and H. J. Trussell, "Optimal color filters in the presence of noise," *IEEE Trans. Image Processing*, vol. 4, no. 6, pp. 814–823, June 1995.
[87] M. Wolski, J. P. Allebach, C. A. Bouman, and E. Walowit, "Optimization of sensor response functions for colorimetry of reflective and emissive objects," *IEEE Trans. Image Processing*, vol. 5, no. 3, pp. 507–517, Mar. 1996.
[88] G. Sharma, H. J. Trussell, and M. J. Vrhel, "Optimal nonnegative color scanning filters," *IEEE Trans. Image Processing*, vol. 7, no. 1, pp. 129–133, Jan. 1998.
[89] D. Travis, *Effective Color Displays: Theory and Practice*. San Diego, CA: Academic, 1991.
[90] W. K. Pratt, "Spatial transform coding of color images," *IEEE Trans. Commun.*, vol. COM–19, no. 12, pp. 980–992, Dec. 1971.
[91] W. B. Pennebaker and J. L. Mitchell, *JPEG Still Image Data Compression Standard*. New York: Van Nostrand, 1993.
[92] J. L. Mitchell, C. Fogg, D. J. LeGall, and W. B. Pennebaker, Eds., *MPEG Digital Video Compression Standard*. New York: Chapman & Hall, 1997.
[93] N. Ahmed and K. R. Rao, *Orthogonal Transforms for Digital Signal Processing*. New York: Springer-Verlag, 1975.
[94] International Radio Consultative Committee, "Encoding parameters of digital television for studios," International Telecommunications Union, Geneva, Switzerland, CCIR Rec. 601–2, 1990.
[95] A. Netravali and B. Haskell, Eds., *Digital Pictures, Representation, Compression, and Standards*. New York: Plenum, 1995.
[96] M. Anderson, R. Motta, S. Chandrasekar, and M. Stokes, "Proposal for a standard default color space for the Internet—sRGB," in *Proc. IS&T/SID 4th Color Imaging Conf.: Color Science, Systems and Applications*, Scottsdale, AZ, Nov. 19–22, 1996, pp. 238–246.
[97] J. C. Zwinkels, "Color-measuring instruments and their calibration," *Displays*, vol. 16, no. 4, pp. 163–171, 1996.
[98] H. R. Kang, *Color Technology for Electronic Imaging Devices*. Bellingham, WA: SPIE, 1997.
[99] J. N. Cook, P. A. Sample, and R. N. Weinreb, "Solution to spatial inhomogenity on video monitors," *Color Res. Appl.*, vol. 18, no. 5, pp. 334–340, Oct. 1993.
[100] International Color Consortium. (Nov. 20, 1995). International Color Consortium profile format, ver. 3.2. [Online]. Available ftp: ftp.fogra.org.
[101] M. C. Stone, W. B. Cowan, and J. C. Beatty, "Color gamut mapping and the printing of digital color images," *ACM Trans. Graph.*, vol. 7, no. 4, pp. 249–292, Oct. 1988.
[102] J. Meyer and B. Barth, "Color gamut mapping for hard copy," in *SID Dig.*, 1989, pp. 86–89.
[103] R. S. Gentile, J. P. Allebach, and E. Walowit, "A comparison of techniques for color gamut mismatch compensation," in *Proc. SPIE Human Vision, Visual Processing, and Digital Display*, B. E. Rogowitz, Ed., 1989, vol. 1077, pp. 342–354.
[104] E. D. Montag and M. D. Fairchild, "Simulated color gamut mapping using simple rendered images," in J. Bares, Ed., *Proc. SPIE Color Imaging Device-Independent Color, Color Hard Copy, and Graphic Arts*, 1996, vol. 2658, pp. 316–325.
[105] ——, "Evaluation of gamut mapping techniques using simple rendered images and artificial gamut boundaries," *IEEE Trans. Image Processing*, vol. 6, pp. 977–989, July 1997.
[106] C. Connolly and T. Fliess, "A study of efficiency and accuracy in the transformation from RGB to CIELAB color space," *IEEE Trans. Image Processing*, vol. 6, pp. 1046–1048, July 1997.
[107] M. D. Fairchild, "Considering the surround in device independent color imaging," *Color Res. Appl.*, vol. 20, no. 6, pp. 352–363, Dec. 1995.
[108] K. M. Braun and M. D. Fairchild, "Testing five color-appearance models for changes in viewing conditions," *Color Res. Appl.*, vol. 22, no. 3, pp. 165–173, June 1997.
[109] International Commission on Illumination, "The CIE 1997 interim color appearance model (simple version), CIECAM97s," Rep. CIE Tech. Committee TC1-34, Aug. 1997.
[110] M. J. Vrhel and H. J. Trussell, "Color correction using principal components," *Color Res. Appl.*, vol. 17, no. 5, pp. 328–338, Oct. 1992.
[111] D. L. MacAdam, Ed., *Sources of Color Science*. Cambridge, MA: MIT Press, 1970.
[112] J. Bares, Ed., *Proc. SPIE Color Imaging: Device-Independent Color, Color Hard Copy, and Graphic Arts*, 1996, vol. 2658.

Gaurav Sharma (Member, IEEE) was born in Dehradun, India, on October 12, 1968. He received the B.E. degree in electronics and communication engineering from the University of Roorkee, India, in 1990, the M.E. degree in electrical communication engineering from the Indian Institute of Science, Bangalore, in 1992, and the M.S. degree in applied mathematics and the Ph.D. degree in electrical engineering from North Carolina State University (NCSU), Raleigh, in 1995 and 1996, respectively.

During 1992–1996, he was a Research Assistant with the Center for Advanced Computing and Communications in the Electrical and Computer Engineering Department at NCSU. Since 1996, he has been a Member of Research and Technical Staff at Xerox Corporation's Digital Imaging Technology Center in Webster, NY. His current research interests include color science and imaging, signal restoration, image halftoning, and error-correction coding.

Dr. Sharma is an associate member of Sigma Xi and a member of the Society for Imaging Science and Technology, the International Society for Optical Engineering, the IEEE Signal Processing Society, and Phi Kappa Phi.

Michael J. Vrhel (Member, IEEE) was born in St. Joseph, MI, in 1964. He received the B.S. degree in electrical engineering from Michigan Technological University, Houghton, in 1987 and the M.S. and Ph.D. degrees in electrical engineering from North Carolina State University, Raleigh, in 1989 and 1993, respectively.

From 1993 to 1996, he was a National Research Council Associate at the National Institutes of Health, Biomedical Engineering and Instrumentation Program. Currently, he is the Senior Scientist at Color Savvy Systems, Ltd., Springboro, OH. His research interests include color reproduction, signal restoration/reconstruction, and wavelets.

Dr. Vrhel received a Kodak Fellowship from Eastman Kodak Company, Rochester, NY, from 1989 to 1993.

H. Joel Trussell (Fellow, IEEE) received the B.S. degree from the Georgia Institute of Technology, Atlanta, in 1967, the M.S. degree from Florida State University, Tallahassee, in 1968, and the Ph.D. degree from the University of New Mexico, Albuquerque, in 1976.

He joined the Los Alamos Scientific Laboratory, Los Alamos, NM, in 1969, where he began working in image and signal processing in 1971. During 1978–1979, he was a Visiting Professor at Heriot-Watt University, Edinburgh, Scotland, where he worked with both the university and industry on image-processing problems. In 1980, he joined the Electrical and Computer Engineering Department at North Carolina State University, Raleigh. During 1988–1989, he was a Visiting Scientist with the Eastman Kodak Company, Rochester, NY. During 1997–1998, he was a Visiting Scientist with Color Savvy Systems, Ltd., Springboro, OH. His research has been in signal and image restoration. Most recently, he has concentrated on accurate measurement and reproduction of color.

Dr. Trussell is a past Associate Editor of IEEE TRANSACTIONS ON ACOUSTICS, SPEECH, AND SIGNAL PROCESSING and is currently an Associate Editor for IEEE SIGNAL PROCESSING LETTERS. He was a member and past Chairman of the Image and Multidimensional Digital Signal Processing Committee of the IEEE Signal Processing Society. He was a member of the Board of Governors of the Signal Processing Society. He was a corecipient of the IEEE Acoustics, Speech, and Signal Processing Society Senior Paper Award in 1986 (with M. R. Civanlar) and the IEEE Signal Processing Society Paper Award in 1993 (with P. L. Combettes).